A NEW APPROACH FOR ENERGY STORAGE AND ELECTROCATALYSIS:

LITHIUM-GAS BATTERIES WITH MOLTEN SALT ELECTROLYTE

by
Hanqian Zhi

A thesis submitted to Johns Hopkins University in conformity with the requirements for the

degree of Master of Science in Engineering

Baltimore, Maryland
May 2020

Abstract

The rapid consumption of fossil fuels in modern society has resulted in a continuously increasing problem of CO_2 emissions, accelerating atmospheric warming, one of the greatest environmental threats. In addition, the risk of fossil fuel depletion is also a challenge that humanity will have to face in the predictable future.

On one hand, the severe situation has thus motivated people to seek for renewable energy source alternatives, such as wind, solar. As a result, the development of efficient electrochemical energy storage and conversion devices, which play a crucial role in storing harvested energies, has become extremely important. On the other hand, in order to mitigate the greenhouse effect, new technologies for CO_2 capture and utilization are urgently needed as well.

In this thesis, a novel molten salt lithium-gas battery system is reported, which has been applied to both Li-O_2 batteries and Li-CO_2 batteries. Li-O_2 batteries are known for high energy density compared to commonly used lithium ion batteries, and the adoption of inorganic molten salt electrolyte and noncarbonaceous nickel-nitrate composite cathode leads to stable cycling, reasonable capacity, good reversibility, and improved electrode kinetics. The feasibility of molten salt electrolyte system is confirmed when extended to Li-CO_2 batteries, based on the achieved good cycling performance and specific capacity. Moreover, the purposed reaction mechanism of Li-CO_2 batteries with discharge products of Li_2CO_3 and carbon is convincingly proved.

Primary Reader and Advisor: Mingwei Chen

Secondary Reader: Chao Wang

Acknowledgements

First, I would like to give my sincere gratitude to Dr. Chao Wang, who provided me with such a precious opportunity to work in a group at the Department of Chemical and Biomolecular Engineering, so that I could continue my research related to batteries. Dr. Wang's profound insights and broad vision in electrochemistry and nanotechnology have been a role model to me. He offered me not only support for research works, but also guidance to my future development. I appreciate all his contributions of time, ideas and financial support.

I am also grateful to my academic advisor, Prof. Mingwei Chen, for always being supportive in my process of degree completion, especially at such a special time of COVID-19 pandemic. As a student working in a group out of the Department of Materials Science and Engineering, I received abundant help from Prof. Chen, without which I would not successfully complete my Master's degree. I would also like to thank my previous academic advisor, Dr. Tim Mueller, who gave me lots of advice on courses registration and projects selection.

Next person I would like to give a specific appreciation is Fei Xu, whom I worked with during the last two years. For me, he is a patient mentor, a reliable colleague, and a considerate friend. I would like to thank other members of Wang Lab who also provided me with generous helps, including Wenqi Zhou, Shiyu Hou, Liyin Zhang, Lanxin Jia, Dr. Lei Wang, Yuxuan Wang, Han Zhang, Han Zong, and Dr. Yifan Liu.

Lastly, I would like to thank Yunjia Song, Mansi Gao and Yang Cheng, my best friends in Hopkins, for all the love and encouragement they provided me in completing my Master's degree. It is lucky for me to have you guys to share all the unforgettable memories.

Contents

List of Tables

List of Figures

1 Introduction

1.1 Energy Crisis and Climate Change

As modern society consumes a huge quantity of energy obtained from non-renewable fossil fuels, the combustion of which pollutes the air and leads to climate change.[1] In the predictable future, the decline of the fossil fuels combined with global warming will be two of the biggest challenges that humanity have to face.[2]

The inevitable fossil fuel depletion[3] and ever-increasing problem of CO_2 emissions therefore motivate people to find ways to obtain energy from renewable alternatives, such as wind, solar and wave.[4] However, since these renewable energy sources are intermittent, the problem of a continuous flow of energy during off peak hours has to be solved. As a result, there is a remarkably increasing need for electrochemical energy conversion and storage devices with high energy and high power density as well as low cost.[3] As common energy storage and conversion technologies, batteries, fuel cells, and supercapacitors have attracted attention from thousands of researchers worldwide.

On the other hand, the increasing concentration of greenhouse gas CO_2 in the atmosphere has caused serious anthropogenic climate changes.[5] To reduce the release of CO_2 into the environment, new technologies for CO_2 capture and utilization are urgently needed, especially ones with value-added products and driven by renewable energy.[6] Thus, various physical and chemical, both photochemical and electrochemical, methods are currently under development for CO_2 conversion.

1.2 Nonaqueous Lithium-Oxygen Batteries

Lithium-ion batteries (LIBs) have become successful and sophisticated devices for high-energy electrochemical storage since their first commercialization in 1991. The capacity of a LIB depends on the amount of Li-ions that can be reversibly extracted from as well as inserted into the structure of electrode materials. For example, in the cathode, which typically limits the overall battery capacity, slightly less than one Li-ion can be stored per transition metal atom. As a result, the active material specific capacity would be 140-200 mAh/g. Therefore, despite the high energy, high power and long life of LIBs, many emerging markets demanding energy densities that may not be achieved by LIBs are seeking for new battery systems. New chemistries, such as lithium-sulfur, magnesium-ion, and lithium-oxygen, are then being explored as high-energy alternatives to LIBs.[7]

In particular, lithium-oxygen (Li-O_2) batteries have received extraordinary research attention in the past decade owing to their potential to provide a high theoretical capacity. Li-O_2 batteries is a kind of metal-air batteries using lithium as the negative electrode, oxygen as the positive electrode reactant, with typically nonaqueous electrolytes.[8] During discharge and charge processes, the reaction mechanism of Li-O_2 batteries is oxygen reduction reaction (OER) upon discharge and oxygen evolution reaction (ORR) on charge.[9]

The nonaqueous Li-O_2 battery was first introduced by Abraham and Jiang[10] in 1996. They suggested that the catalytic reduction of oxygen is mostly lithium peroxide (Li_2O_2) formation via a two-electron process.

$$2(\mathrm{Li^+ + e^-}) + \mathrm{O_2} \leftrightarrow \mathrm{Li_2O_2}$$

with the forward direction describing discharge and the reverse direction describing charge. The standard potential of Li_2O_2 formation (and decomposition) is U_0 = 2.96 V (with respect to Li/Li^+). Although the mechanism of Li-O_2 batteries is still controversial, this theory is now widely accepted.

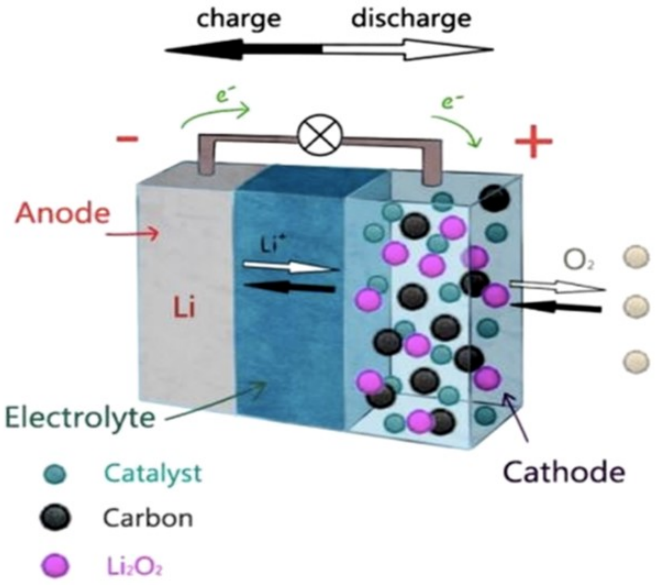

Fig. 1-1 . Working principle of a lithium-oxygen battery.[8]

Besides, irreversible reactions forming lithium oxide have been suggested to contribute to the cathode chemistry during deep discharges.[11]

$$4(\mathrm{Li^+ + e^-}) + \mathrm{O_2} \longrightarrow 2\mathrm{Li_2O} \qquad U_0 = 2.91\ \mathrm{V}$$

$$\mathrm{Li_2O_2} + 2(\mathrm{Li^+ + e^-}) \longrightarrow 2\mathrm{Li_2O} \qquad U_0 = 2.72\ \mathrm{V}$$

Many studies have reported extended discharge-charge cycles with modest loss in capacity, most of which are based on coulometry, that is, by tracking the loss of discharge capacity with

repeated discharge-charge cycles. This approach assumes that chemical reaction with Li_2O_2 formation describes the fundamental processes occurring in both cell discharge and charge, with a secondary parasitic process describing the capacity loss. However, there is still lack of quantitative experimental evidence, which definitively proves that the first reaction above is the dominant reversible electrochemical process in Li-O_2 batteries.[12]

In fact, multiple publications have hinted that the Li-O_2 electrochemistry may be substantially more complicated than a simple combination of the three reactions mentioned above. Using cyclic voltammetry, Laorie et al. have shown that the choice of solvent has a significant influence on fundamental processes occurring during ORR and OER in the presence of Li-ions.[13]

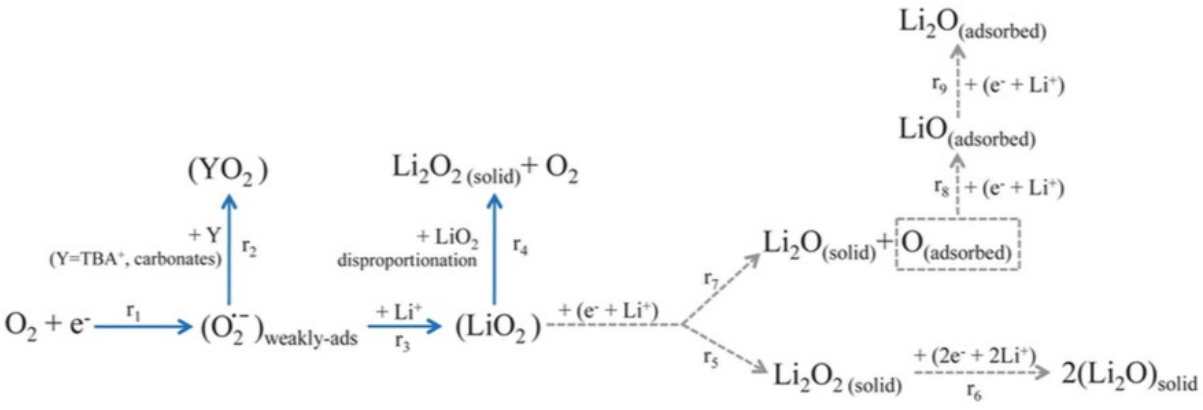

Fig. 1-2. Reaction scheme of oxygen reduction reaction in nonaqueous media.[8]

It has been well established that ORR in nonaqueous solvents with large cations such as tetraethylammonium (TEA^+) and tetrabutylammonium (TBA^+) proceeds by a one-electron transfer to form the superoxide ion (O_2^-) as an intermediate species (r_1 in Fig. 1-2), while the

formation of peroxide (O_2^{2-}) was not observed. The kinetics of the O_2/O_2^- redox couple, with an equilibrium voltage of ~2.0 V, was found to be fast and reversible. In contrast, the replacement of large cations (e.g., TBA^+) with smaller metal cations (e.g., Li^+) leads to a positive shift of the thermodynamic equilibrium potential as a result of changing the redox couple from $O_2/(O_2^-–TBA^+)$ to $O_2/(O_2^-–Li^+)$. This step can be followed by disproportionation to metal peroxide and O_2.

Such significant changes in ORR thermodynamics between large cations and smaller metal cations can be rationalized using hard soft acid base (HSAB) theory. According to HSAB, as a soft acid, TBA^+ can effectively stabilize the soft base, O_2^- (due to its relatively large radius and low charge density), preventing further reactivity. However, alkali metal cations such as Li^+, which are hard acids, cannot effectively stabilize O_2^-. Therefore, a disproportionation (r_4 in Fig. 1-2) or a second electron transfer reaction (r_5 in Fig. 1-2) to Li_2O_2 from the unstable LiO_2 is favored in the presence of Li-ions.[9]

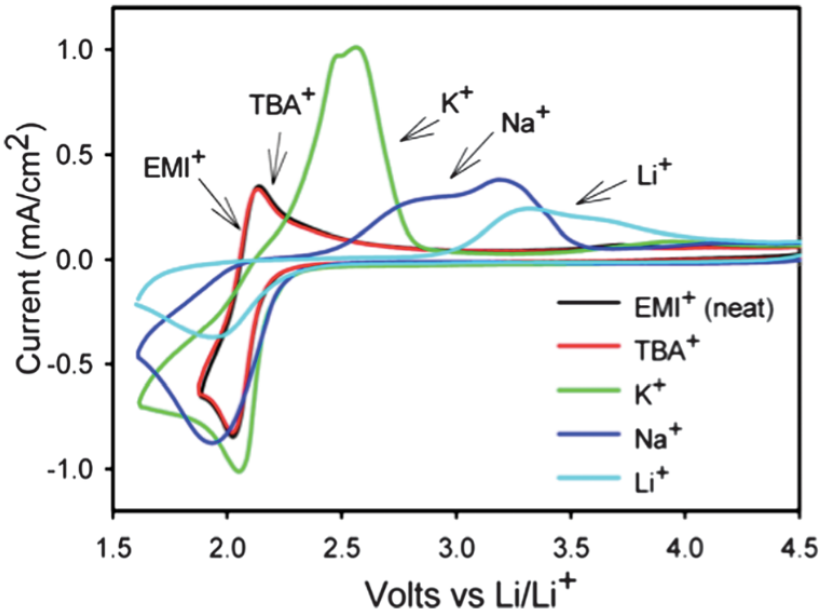

Fig. 1-3. CVs of neat EMITFSI along with various salts at 0.025 M concentration on a GC electrode at 100 mV s^{-1}.[14]

Allen and co-workers[14] have applied HSAB to the study of ORR and OER processes using a series of cations with increasing Lewis acidity (i.e., cation hardness): $TBA^+ < PyR^+ < EMI^+ < K^+ < Na^+ < Li^+$ (Fig. 1-3). It was shown that the superoxide ions can be effectively stabilized by TBA^+, PyR^+, EMI^+ and K^+ cations without disproportionate to form peroxide, which enables reversible one-electron reactions. In contrast, hard cations such as Li^+ and Na^+ promote the disproportionation of metal superoxide to form metal peroxide, yielding an irreversible two-electron process.

In addition, the HSAB theory coupled with the relative stabilities of the Li^+–$(solvent)_n$ complexes existing in different solvents can also provide a reasonable explanation for the different O_2 reduction products formed in Li^+-conducting electrolyte solutions. High donor numbers (DN) solvents improve stability for the complex $[Li^+(solvent)_n–O_2^-]$ because of the modulated Lewis acidity of the hard acid. In such electrolytes, a distinct O_2/O_2^- reversible couple may be seen in the presence of Li^+. In solvents with low DN, the general tendency for O_2^- is to undergo a quick decomposition or a fast electrochemical reduction to O_2^{2-}. In Li^+ electrolytes prepared in low DN solvents, O_2 may be fully reduced to O^{2-}.[13]

1.3 Molten Salt Lithium-Oxygen Batteries

As described above, the mechanism of conventional Li-O_2 batteries is confusing due to the impact from electrolytes and solvents. In order to fully understand the reactions, ORR and OER, happening during the charge and discharge processes of Li-O_2 batteries, a distinct mechanism is of great necessity. Therefore, we expect to find alternatives to these disturbing organic

electrolytes which are usually volatile, unstable and air-intolerant as well. In addition, the elements contained in these organic electrolytes could lead to unwanted side reactions and thus affect the detection of products generated during cycling.

A novel Li-O_2 battery system employing alkali metal nitrate molten salt as inorganic electrolyte was first demonstrated by Giordani *et al.*[7] In fact, researches on molten nitrate electrolytes for lithium batteries and thermal batteries trace back to the late 1970s.[15] It was observed that the SEI, composed of Li_2O, generated through the reaction between lithium metal and the nitrate anion was sufficiently stable for primary cells and rechargeable cells with limited cycle life. However, few works have been done on O_2 electrode behavior in such electrolytes before. It was also reported that equilibria between superoxide, peroxide and oxide forms of reduced oxygen could coexist in the molten salt electrolyte with high reversibility at a Pt rotating disk electrode (RDE),[16,17] so that the foundation for molten salt Li-O_2 batteries was laid. Besides, all these outstanding features, including the stability toward Li, low melting point relative to other inorganic salts, high thermal stability above 500 °C, nonvolatility, high ionic conductivity and acceptable electrochemical stability window, make the molten nitrates promising electrolytes for Li-O_2 batteries.

Giordani *et al.* reported an intermediate temperature Li-O_2 battery using a lithium metal anode, a molten nitrate-based electrolyte and a porous carbon (Super P carbon) O_2 cathode. They found that eutectic molten nitrate salt mixtures, such as $LiNO_3$-KNO_3 (melting point: ~125 °C) and $LiNO_3$-KNO_2-$CsNO_3$ (melting point: ~90 °C) are currently the most stable Li^+-bearing electrolytes known for the reversible oxygen electrochemistry occurring at the Li-O_2 battery

cathode. The specific properties of these two kinds of electrolytes are listed in Table 1-1.

Table 1-1. Molten salt electrolytes used in Giordani *et al.*'s work[7]

electrolyte	chemical composition (mol %)	melting point (°C)	Li^+ transference number	ionic conductivity (mS/cm, 150 °C)
$LiNO_3$-KNO_3	42−58	125	0.68	88
$LiNO_3$-KNO_2-$CsNO_3$	37−39−24	90	0.28	115

Corresponding to the different eutectic point of electrolyte systems, the battery was operated at 120 and 150 °C with binary and ternary mixtures of alkali metal nitrates respectively. It has been proved by RDE measurements and SEM that the elevated temperature needed for molten salts leads to enhanced solubility of the discharge products, LiO_2 and Li_2O_2, in the electrolytes compared to room-temperature organic electrolytes. Together with improved electrode kinetics, high reversibility and higher rate capability were demonstrated for the O_2 electrode.

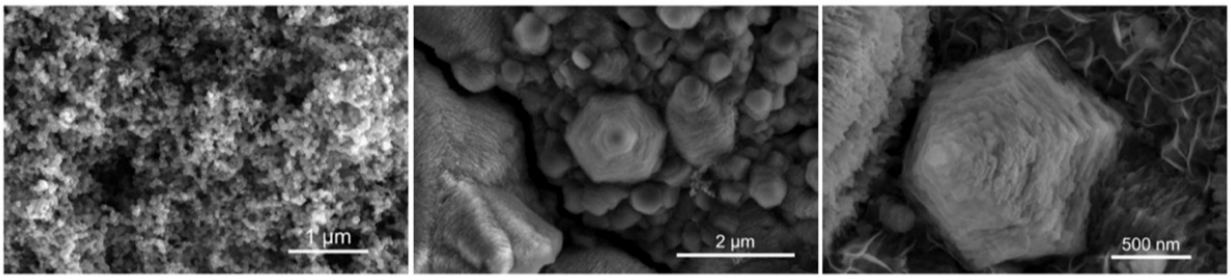

Fig. 1-4. SEM images of the Super P carbon O_2 electrode. From left to right: electrode before discharge (Super P carbon nanoparticles) and electrode following a ~1400 mAh/g discharge under O_2 to cutoff voltage of 2.6 V (Li_2O_2 particles).[7]

The SEM images of the Super P carbon O_2 electrode (Fig. 1-4) show the formation of Li_2O_2, as the hexagonal shape of deposited Li_2O_2 was observed. This means ORR in $LiNO_3$-KNO_3 molten salt Li-O_2 battery is based on a 2 e^-/O_2 process which generates Li_2O_2 as the discharge product. The reversible formation of crystalline Li_2O_2 was confirmed by XRD (Fig. 1-5b), while *in-situ* gas and pressure analysis (Fig. 1-5a) indicated that oxygen could be efficiently evolved during charge at a very low overpotential, with a discharge/charge voltage gap of only ~0.1 V.

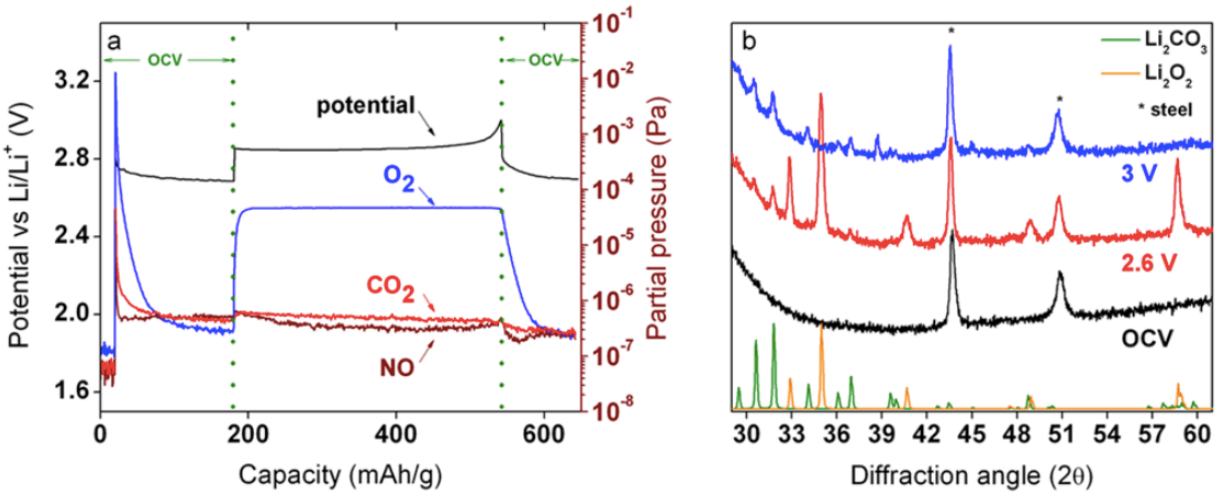

Fig. 1-5. (a) Li-O_2 battery charging profile with *in-situ* gas analysis. Battery employed a $LiNO_3$-KNO_3 molten salt electrolyte, a Super P carbon:PTFE cathode, and was charged at 150 °C, ~80 mA/g, to a 3.0 V cutoff. Capacity expressed in mAh/g of carbon. (b) XRD analysis of a Super P carbon cathode following an OCV period (before discharge), a single discharge to 2.6 V, and a discharge/charge cycle between 2.6 and 3.0 V, in $LiNO_3$-KNO_3 molten salt electrolyte at 150 °C.[7]

Compared to typical organic electrolyte (0.1 M $LiClO_4$-DMSO), the Li-O_2 battery using $LiNO_3$-KNO_2-$CsNO_3$ molten salt electrolyte showed remarkably low voltage hysteresis (~0.1 V) and good

capacity retention according to the cycling data. Fig. 1-6a,b are the cycling curves, while Fig. 1-6c,d depict the O_2 partial pressure monitoring of Li-O_2 batteries with different kinds of electrolyte. Fig. 1-6c clearly shows that only a small fraction of O_2 consumed during discharge is evolved during charge. Side reactions govern the electrochemistry in the DMSO-based battery, resulting in rapid capacity fade shown in Fig. 1-6a.

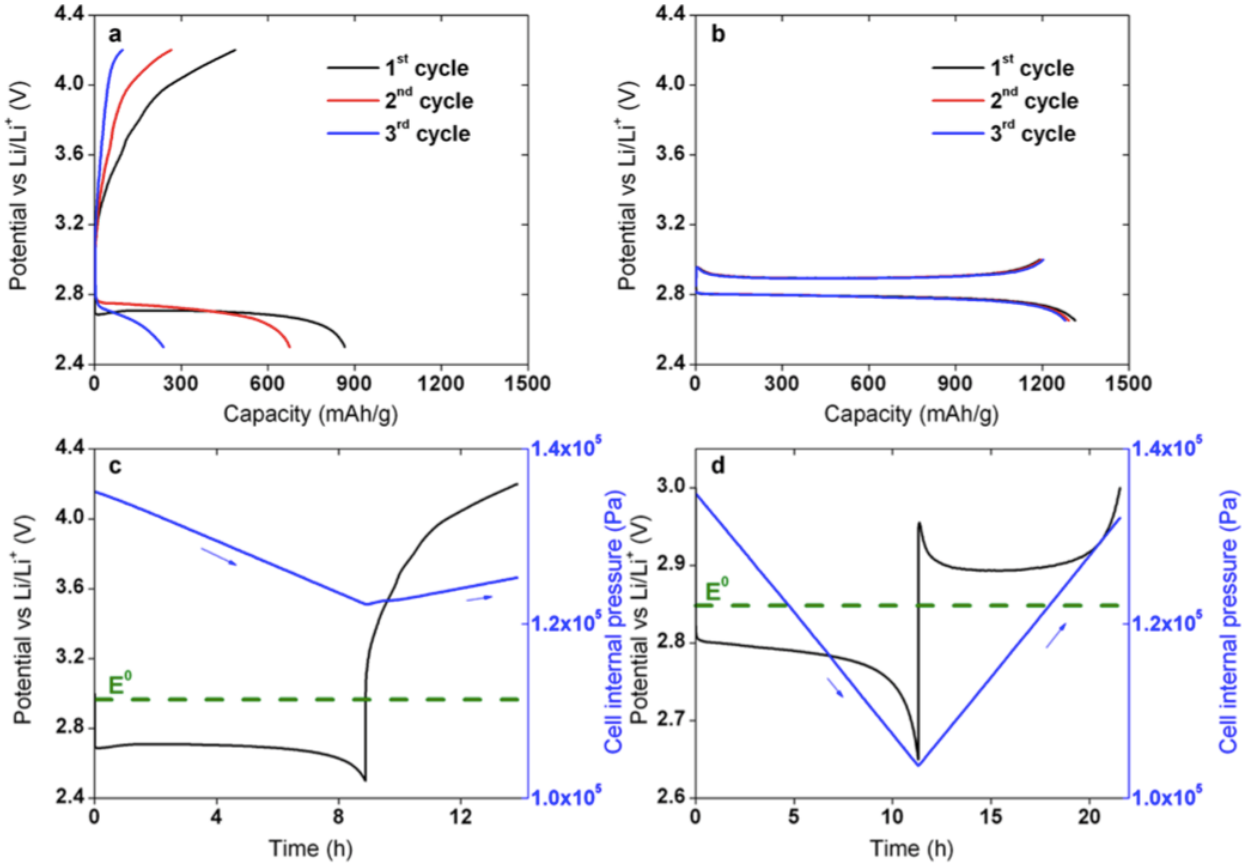

Fig. 1-6. Li-O_2 battery voltage and pressure profiles measured in (a,c) 0.1 M $LiClO_4$-DMSO at 30 °C between 2.5 and 4.2 V and (b,d) $LiNO_3$-KNO_2-$CsNO_3$ molten salt electrolyte at 120 °C between 2.65 and 3.0 V. Positive electrode: Super P carbon:PTFE 95:5 wt %, current: 0.25 mA (~80 mA/g carbon). Electrolyte loading: 150 μL. Carbon loading: ~4 mg/cm^2.[7]

However, despite all these impressive advantages of this molten salt Li-O_2 battery system, some imperfections remain to be improved. For example, the authors found that Super P carbon, which was used as the cathode material, tended to react with oxygen reduction products to form the by-product lithium carbonate (Li_2CO_3). They also demonstrated that decomposition of the amorphous carbon electrode could cause battery failure. Therefore, it was purposed that the identification of suitable noncarbonaceous cathode materials will be key to success for this chemistry.[7]

Following Giordani's work, Karkera and Prakash[18] realized stable cycling, low overpotential and high rate capability in the Li-O_2 battery employing $LiNO_3$-KNO_2-$CsNO_3$ (37:39:24) eutectic salt mixture as electrolyte, and confirmed that the use of molten salt electrolyte would significantly eliminate the side reactions during charge-discharge process.

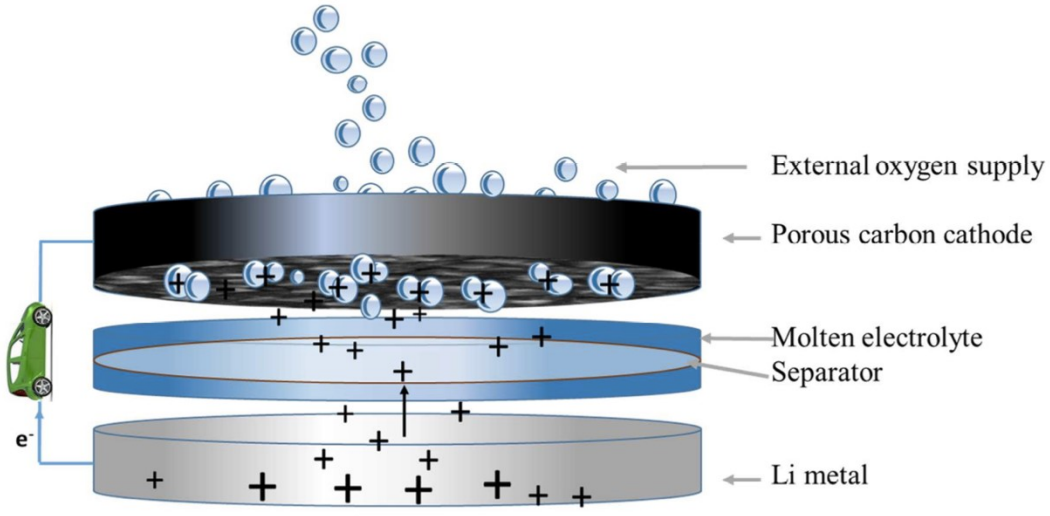

Fig. 1-7. Schematic representation of a molten salt electrolyte Li-O_2 battery at discharged condition.[18]

The battery was assembled as Fig. 1-7, which is same as the setup in Giordani's work, and

operated at 140 °C. The CV of molten salt Li-O_2 battery (Fig. 1-8a) indicates that the area under the curve for cathodic peak (2.7 V) and anodic (2.85 V) peak, as well as the peak currents ($ip_a/ip_c \approx 1$), are almost equal, suggesting a highly reversible chemical process. The distinct peaks were interpreted as the generation of superoxide anion ($O_2^{\cdot-}$) and its oxidation in reverse scan. In contrast, the CV performed in the presence of Ar gas (red curve, Fig. 1-8b) only results in background currents.

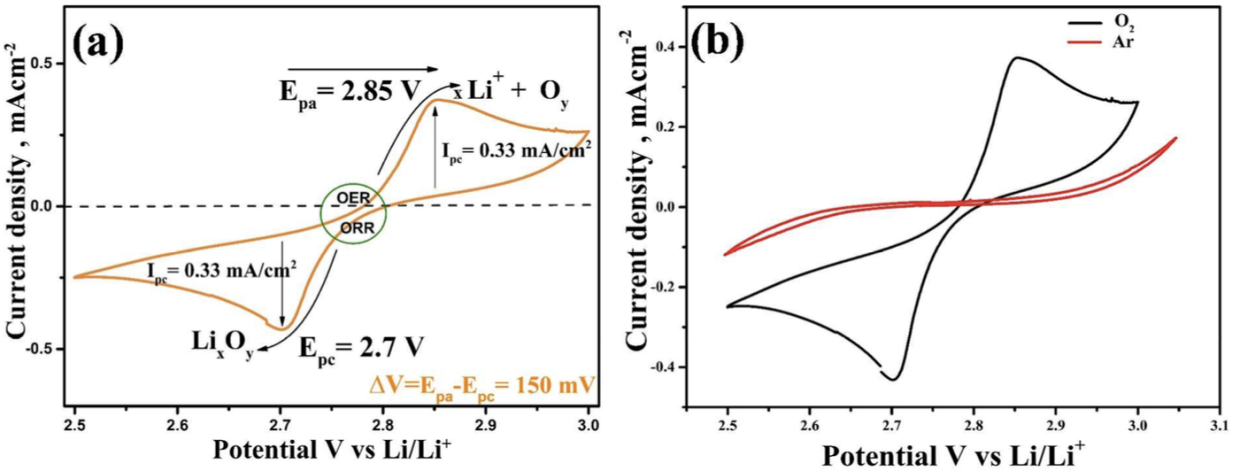

Fig. 1-8. (a) Cyclic voltammograms obtained from Vulcan carbon:PVDF electrode molten electrolyte Li-O_2 battery at 140 °C, (b) CV in O_2 saturated electrolyte (black) and Ar saturated electrolyte (red), Working electrode: Vulcan carbon, carbon loading ~1 mg/cm^2. Counter and reference electrodes: Li metal. Scan rate: 0.1 mV/s. Voltage window: 2.5−3.0 V. Current density expressed in mA/g of carbon.[18]

Fig. 1-9 shows the rate performance of the Li-O_2 cell at different current densities. With current densities from 0.1 mA/cm^2 to 4 mA/cm^2, the corresponding voltage hysteresis shown in charge-discharge cycles varied from 40 mV to 0.85 V. The current density of 3 mA/cm^2 is about 100 times higher than that applied in conventional nonaqueous Li-O_2 batteries. In addition, for

the 40 mV overpotential case, the round-trip energy efficiency of discharge-charge cycle is close to 98%, which is much higher than the requirement that practical battery systems should exhibit round-trip energy efficiencies above 90%. They explained that compared to organic electrolytes and ionic liquids, the elevated temperature needed for molten salt electrolyte could overcome the high rate operation challenge of Li-O_2 battery, because the rate of reaction is directly proportional to the temperature.

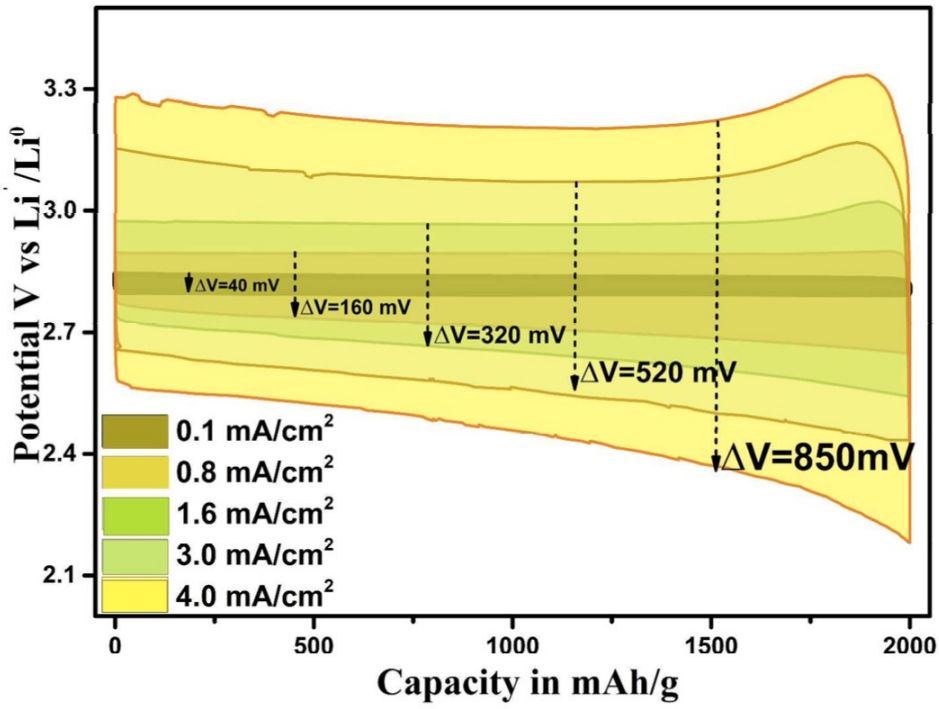

Fig. 1-9. The rate performance of Li-O_2 battery in $LiNO_3$-KNO_2-$CsNO_3$ (37:39:24) electrolyte at 140 °C at current density ranges 0.1-4.0 mA/cm^2 in voltage window 2-3.4 V.[18]

XRD and FESEM were used to determine the discharge products. The diffraction patterns indicate that the discharge product is primarily Li_2O_2, which is not observed during charge (Fig. 1-10a), confirming the reversibility of the charge-discharge process as suggested by the CV

experiments. The discharged electrolyte (Fig. 1-10c) additionally had Li_2O reflections, which is also not observed during charging (Fig. 1-10d). This indirectly reveals that Li_2O formed during discharge with the nitrate reduction process, becoming a protective layer on Li anode. The appearance of Li_2O_2 and Li_2O was confirmed by FESEM images (Fig. 1-11). The abundant hexagonal and octahedral shaped crystals on discharged cathode should be Li_2O_2 and Li_2O respectively, according to several theoretical studies[19,20]. Same as the XRD result of $LiNO_3$-KNO_3 system in Giordani's article, small traces of Li_2CO_3 are seen on cathode (marked as *) which probably due to the reaction of carbon in cathode with Li_xO_y (x=1, 2; y=1, 2). As the auto oxidation of commonly used organic electrolyte would create the passivating layer on electrodes, leading to the failure of Li-O_2 batteries,[21,22] Li metal cycled in molten salt electrolyte rich in $LiNO_3$ (> 350 hrs) showed unchanged Li phase with additional peaks of Li_2O, Li_3N and KNO_3 (Fig. 1-10e). The undesired by-product LiOH was not observed, while Li_3N, the good conductor of Li-ion and also the protective layer like Li_2O, was formed through the electrochemical/chemical reaction of Li with by-products of nitrate-nitrite interconversion.

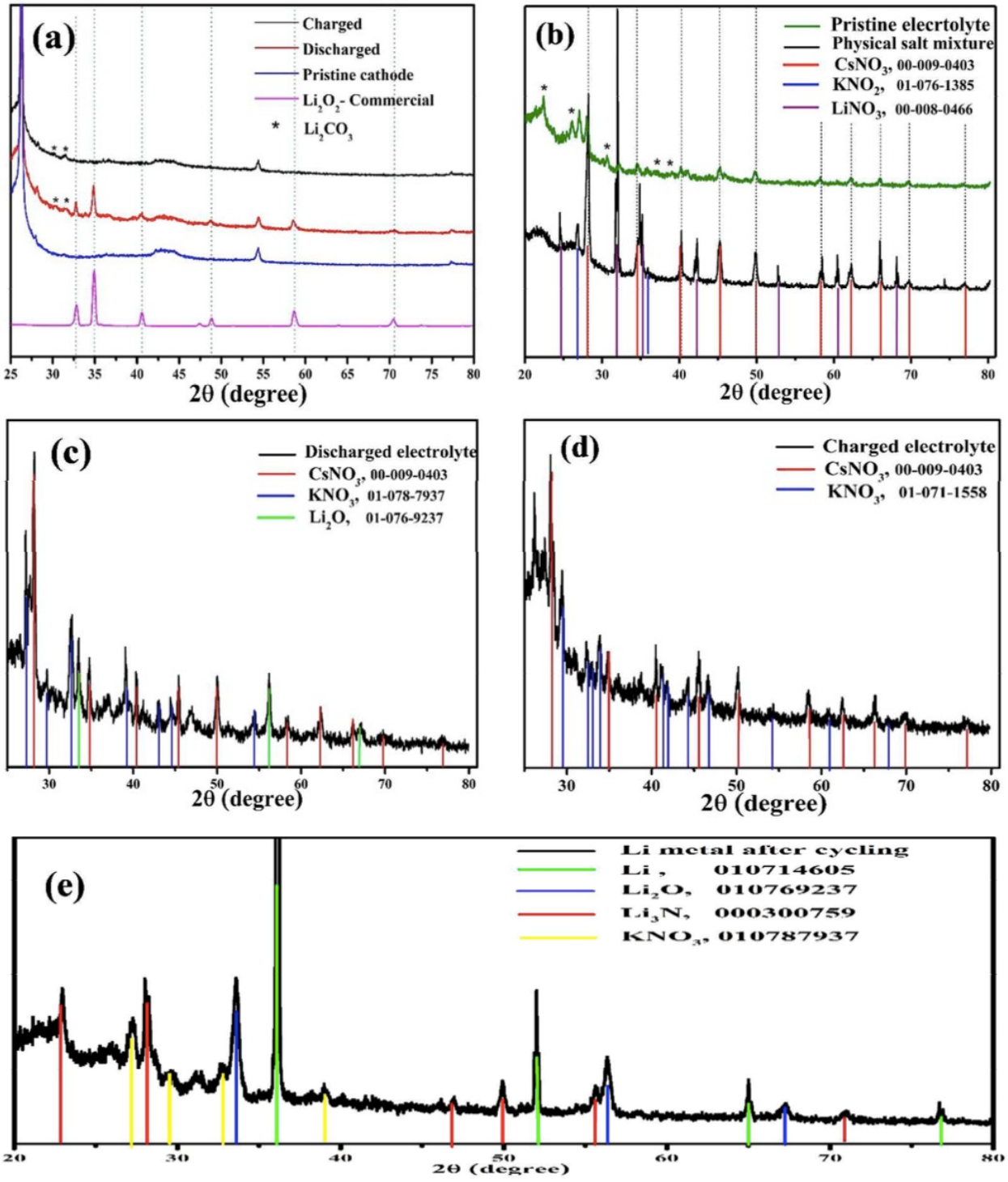

Fig. 1-10. *Ex-situ* XRD patterns of (a) Vulcan carbon cathode; (b) Pristine electrolyte compared with physical mixture; (c) discharged electrolyte; (d) charged electrolyte; (e) anode after cycling in $LiNO_3$-KNO_2-$CsNO_3$ (37:39:24) electrolyte Li-O_2 battery.[18]

Based on these characterization results, the authors purposed a possible mechanism of molten salt electrolyte Li-O_2 batteries, which is slightly different from that of conventional nonaqueous batteries. it first involves a reversible nitrate-nitrite interconversion (the first equation below) to form Li_2O layer on Li metal (the second equation). Then is the formation, growth and consequent decomposition of Li_2O_2 during a complete charge-discharge cycle (the third equation).[18]

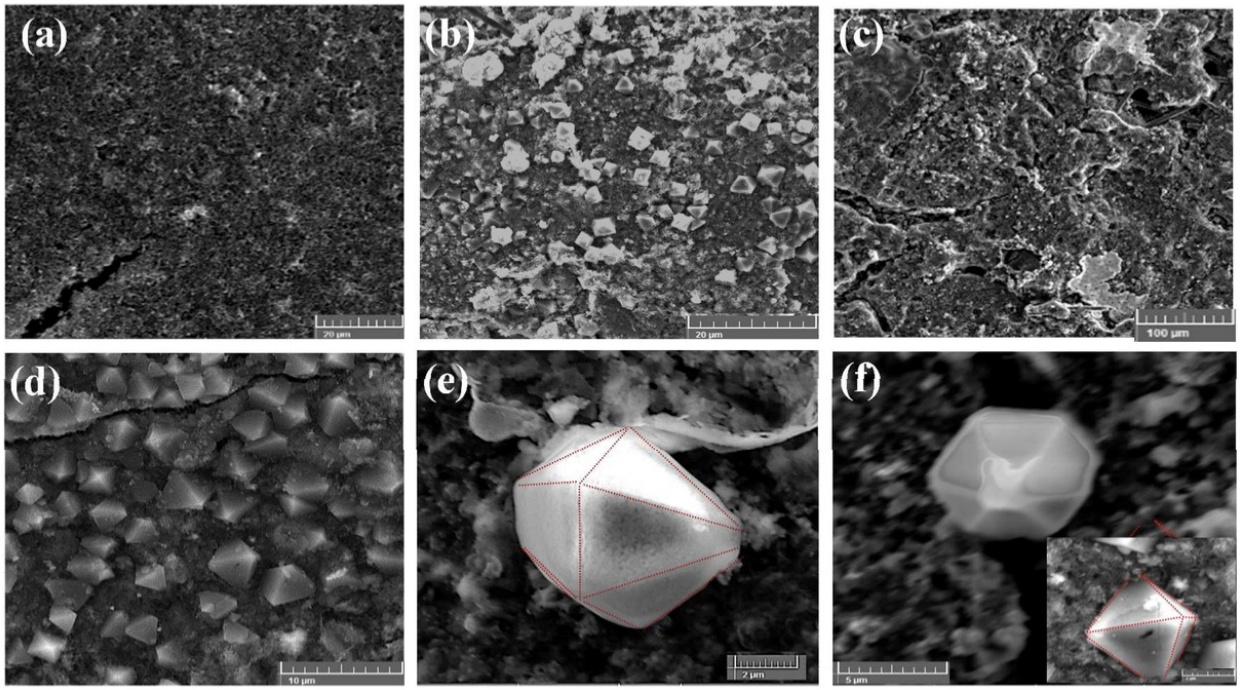

Fig. 1-11. Field emission SEM images of VC:PVDF O_2 cathode: Low magnification images of (a) pristine, (b) discharged, (c) charged electrodes. (d-f) Higher resolution images of discharged cathode.[18]

$$LiNO_3 \leftrightarrow LiNO_2 + {}^1/_2\, O_2$$

$$2(Li^+ + e^-) + {}^1/_2\, O_2 \longrightarrow Li_2O$$

$$2(Li^+ + e^-) + O_2 \leftrightarrow Li_2O_2$$

However, the carbon cathode is still a problem left, as carbon corrosive was evidenced in both $LiNO_3$-KNO_3 and $LiNO_3$-KNO_2-$CsNO_3$ electrolytes Li-O_2 batteries. In 2018, Xia *et al.*[23] reported a molten salt Li-O_2 battery based on a reversible four-electron conversion to Li_2O, in which a noncarbonaceous composite cathode composed of nickel nanoparticles was used.

The authors introduced an unique viewpoint that In comparison with Li_2O_2, which is believed to be the main discharge product of Li-O_2 batteries, Li_2O is much less chemically reactive with organic solvents and with carbon cathode. Because Li_2O is benign as an oxidizing agent due to its oxide anion. More importantly, a theoretically higher specific energy and energy density will be delivered if Li-O_2 batteries work based on Li_2O as the discharge product. Therefore, they found a new pathway for reversible oxygen reduction to the oxide in this article.

Nevertheless, the problem of this idea is that the formation of Li_2O, instead of Li_2O_2, is neither dynamically nor kinetically favored at ambient conditions. Form thermodynamic perspective, the standard Gibbs reaction energy of forming Li_2O_2 from Li and O_2 is lower than that of Li_2O, according to the equations below.

$$2\mathrm{Li} + \mathrm{O_2} \rightarrow \mathrm{Li_2O_2} \;\; \Delta_r G^0 = -571 \text{ kJ mol}^{-1}$$

$$2\mathrm{Li} + 0.5\mathrm{O_2} \rightarrow \mathrm{Li_2O} \;\; \Delta_r G^0 = -561 \text{ kJ mol}^{-1}$$

Considering kinetic conditions, the formation of Li_2O requires O-O bond cleavage of O_2 molecules, whereas peroxide does not. Therefore, special approaches must be adopted to overcome these intrinsic barriers.

Fortunately, the increased operation temperature and stable inorganic electrolyte in molten salt Li-O_2 batteries are all ideal factors for the reversible formation of Li_2O. As the Li-O_2 cells were

cycled at 150 °C, the thermodynamic driving force favors Li_2O as the discharge product above this temperature rather than Li_2O_2 (Fig. 1-12a), and the $LiNO_3$-KNO_3 eutectic molten salt used as electrolyte could deliver good chemical stability and high conductivity.[7] To solve the problem of O-O bond cleavage and formation, a composite cathode composed of nickel nanoparticles and nitrates, instead of carbonaceous cathode, was employed to supply the vital electrocatalyst that reversibly catalyzes O-O bond reactions.

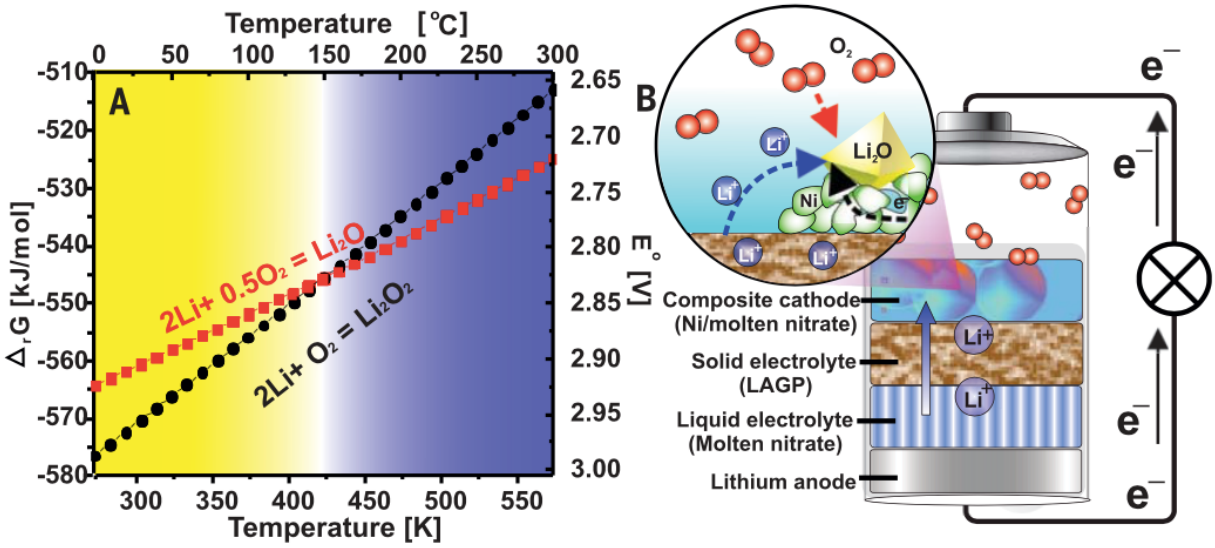

Fig. 1-12. (a) Gibbs reaction energy for formation of Li_2O and Li_2O_2 as a function of temperature. (b) Configuration of the molten salt Li-O_2 cell and schematic illustration of Li_2O formation during discharge.[23]

The cell design is depicted in Fig. 1-12b. Besides the typical Li-O_2 battery components, a solid electrolyte [$Li_{1.5}Al_{0.5}Ge_{1.5}(PO_4)_3$ (LAGP)] membrane was added at the Li anode, which could inhibit the crossover of soluble by-products, such as Li_2CO_3, $LiNO_2$ and Li_2O.

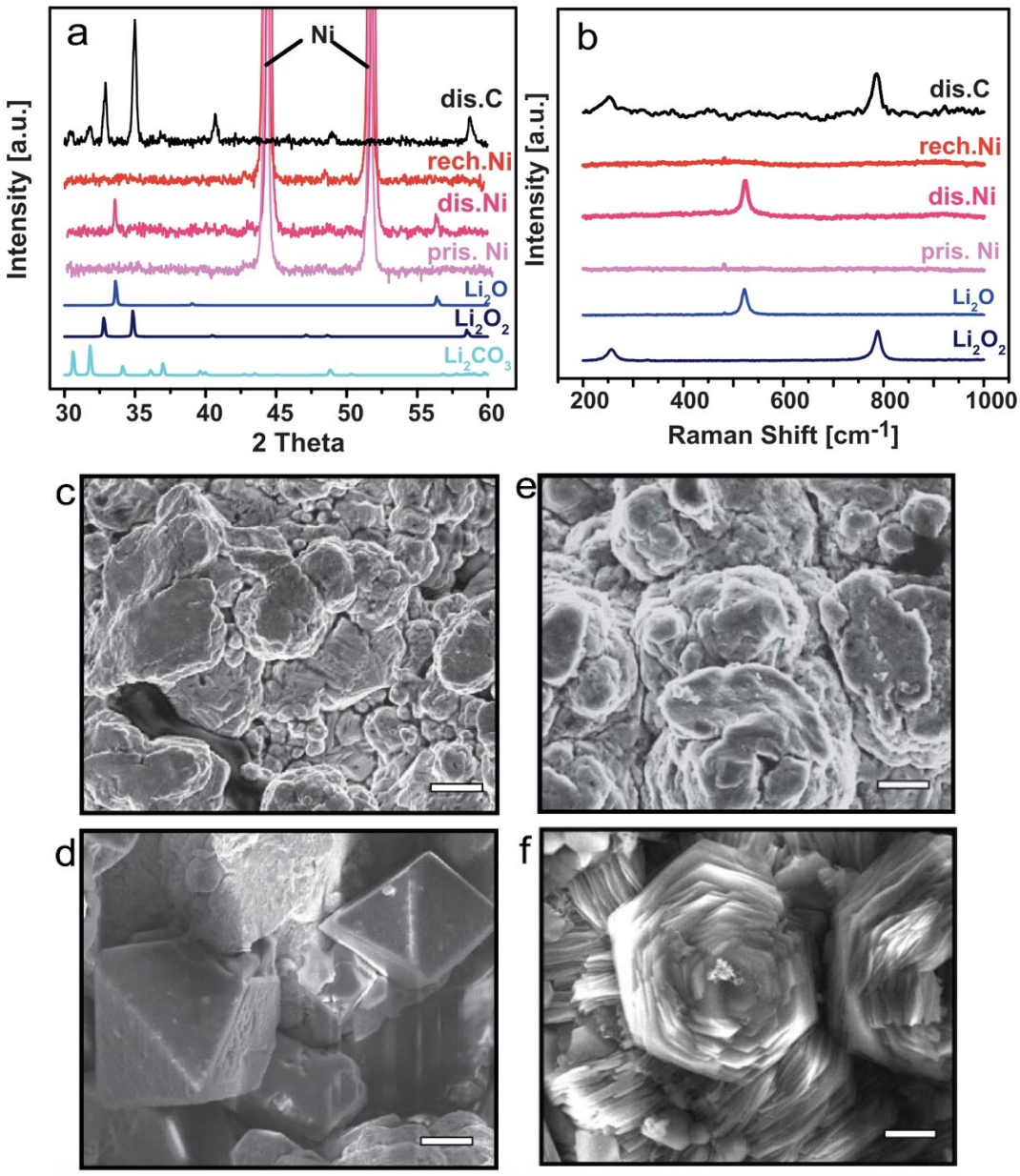

Fig. 1-13. Characteristics of Li-O_2 cells using carbon and Ni-nitrate composite cathodes. (a) XRD patterns, (b) Raman spectra, and SEM images of (c) pristine Ni cathode, (d) Ni cathode discharged to 2.6 V then (e) recharged to 3.5 V, and (f) carbon cathode discharged to 2.6 V. Scale bars, 2 μm.[23]

The products generated during charge-discharge were examined by XRD, Raman analysis and SEM. After fully discharging the cell to 2.6 V, the XRD pattern of the composite cathode

showed two peaks assigned to the (111) and (022) reflections of Li_2O (Fig. 1-13a). The formation of Li_2O was further supported by the Raman band definitive of Li_2O at 523 cm^{-1} (Fig. 1-13b). Furthermore, the SEM image in Fig. 1-13d revealed that the discharged cathode was covered with large octahedral crystals, the morphology of Li_2O. The disappearance of Li_2O in the XRD pattern (Fig. 1-13a) and Raman spectrum (Fig. 1-13b) of the recharged cathode indicated that Li_2O had been fully removed by oxidation. In addition, the charged cathode in Fig. 1-13e was bare as that before discharge (Fig. 1-13c), with no crystal structures observed, showing excellent electrochemical reversibility of the inorganic electrolyte Li-O_2 cell with a Ni-nitrate composite cathode. In contrast, under same conditions, Li_2O_2 was identified as the main discharge product in the Super P carbon electrode cell, according to the XRD and Raman analysis (Fig. 1-13a,b, black curves). Identical to the results in the previous two articles, hexagonal-shaped Li_2O_2 crystal was also detected by SEM (Fig. 1-13f).

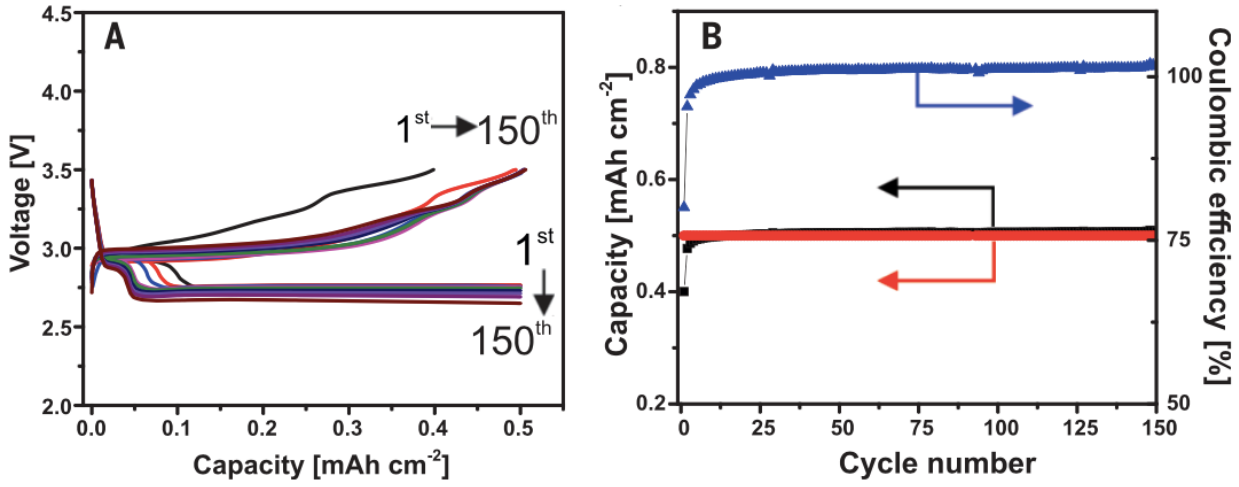

Fig. 1-14. Cycling performance of a molten salt electrolyte Li-O_2 cell with a Ni-nitrate composite cathode. (a) Discharge and charge curves over 150 cycles at a constant current of 0.2 mA/cm^2. (b) The corresponding

changes of discharge capacity (red), charge capacity (black), and CE (blue) during cycling.[23]

The Ni-nitrate cathode Li-O_2 cell was cycled with a limited capacity of 0.5 mAh/cm^2 at 0.2 mA/cm^2 for 150 cycles (Fig. 1-14a). The cycling curves exhibited two discharge plateaus, the first at 2.9 V corresponding to a very low capacity, followed by a much longer discharge plateau at 2.7 V. The first plateau is ascribed to initial formation of the Li_2O species in solution, while the longer plateau at 2.7 V corresponds to oxygen reduction at the surface of the catalyst to form Li_2O. Upon charge, the cell exhibited two charge plateaus at 3.0 V and 3.3 V. It is speculated that the first plateau at 3.0 V is due to the oxidation of Li_2O crystallites that are deposited near or on the catalyst at the cathode, whereas the higher plateau at 3.3 V corresponds to the oxidation of Li_2O deposited on LAGP. Fig. 1-14b indicated that the coulombic efficiency (CE) of the cell increased rapidly from 80 to 100% over four cycles and is subsequently stable.

The authors then proposed a peroxide-mediated ORR pathway to explain the mechanism of this battery system, which is illustrated in Fig. 1-15 and outlined below.

Diffusion: Upon discharge, oxygen adsorbs on the surface of the cathode.

$$O_2 \longrightarrow O_{2,ad}$$

Reduction: Via a two-electron transfer, oxygen is electrochemically reduced to $Li_2O_{2,ad}$, on the surface of the catalyst.

$$O_{2,ad} + 2e^- + Li^+ \longrightarrow Li_2O_{2,ad}$$

Desorption: A small amount of $Li_2O_{2,ad}$ slowly desorbs from the catalyst surface due to its low solubility and diffusibility in the molten nitrate electrolyte.

$$Li_2O_{2,ad} \longrightarrow Li_2O_{2,electrolyte}$$

Disproportionation: The major remaining Li_2O_2 is converted to Li_2O by the catalyst through disproportionation.

$$Li_2O_{2,ad} \rightleftarrows Li_2O_{ad} + {}^{1}/_{2}\, O_2$$

Transport: Once formed, Li_2O is soluble in the molten salt electrolyte, and on supersaturation formation of Li_2O nuclei triggers nucleation and growth, resulting in micrometer-sized Li_2O crystals.[24]

$$Li_2O_{ad} \longrightarrow Li_2O_{electrolyte}$$

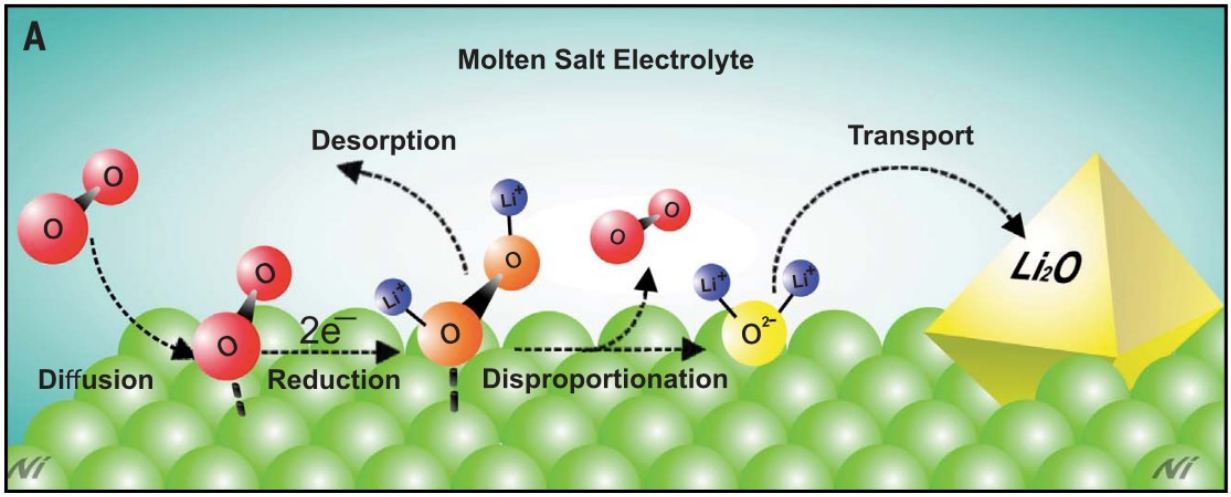

Fig. 1-15. Schematic illustration of the pathway of the oxygen reduction reaction over the Ni-based composite catalyst.[23]

In conclusion, this prominent work directly addressed a number of issues related to Li-O_2 chemistry by tuning the operating temperature and using a single bifunctional ORR/OER catalyst, the *in-situ* generated Li_xNiO_2 electrocatalyst at the composite cathode. The four-electron transfer

from Li_2O was proven to be possible, reversible, and not intrinsically limited, which could operate with almost theoretical CE. Moreover, the authors purposed that this "Li_2O" cell could combine with other electrochemical devices, such as fuel cells and electrolyzers, which also operate on the basis of a 4 e^- process, developing a simple reversible energy storage system.[23]

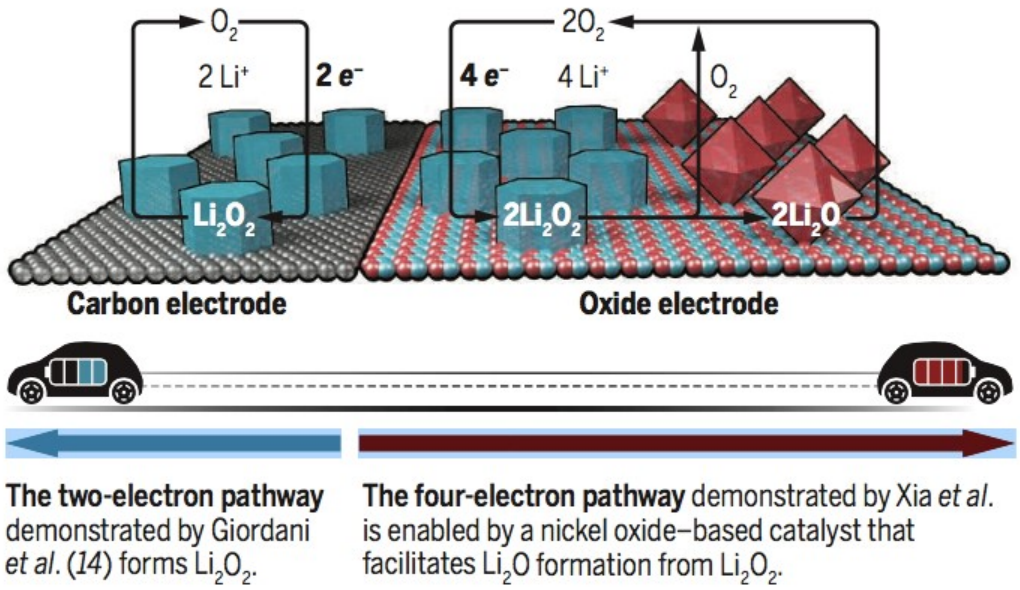

Fig. 1-16. Two types of rechargeable Li-O_2 battery chemistries operate at high temperatures (150 °C) and take advantage of molten salt electrolytes.[25]

Feng *et al*. summarized the two routes suggested for molten salt electrolyte Li-O_2 batteries (Fig. 1-16), and also purposed the challenges this new chemistry is facing.[25] As still little is known about the reaction mechanism for the oxygen electrode in such high-temperature molten salt electrolyte environments, efforts are needed to figure out the atomistic understanding. In addition, the four-electron pathway highlights the opportunities to develop catalysts that could improve the kinetics and selectivity of oxide formation, as well as to design the catalysts and

electrode surfaces against peroxide and oxide to achieve long cycle life. Furthermore, this issue urges the development of light, transition metal-free, electrically and ionically conductive porous structures, which are required to host the catalyst, to enable reversible oxidation, and to stabilize the lithium-electrolyte interface during cycling.

1.4 Lithium-CO_2 Batteries

Besides Li-O_2 batteries, another kind of lithium-gas electrochemical technology, Li-CO_2 batteries, is also continuously attracting researchers' interest as a promising new approach for CO_2 capture and energy storage.[26] Since CO_2 is accelerating atmospheric warming as a predominant greenhouse gas, how to realize eco-efficient and environment-friendly CO_2 fixation has become one of the major global challenges to cope with the climate change. However, despite the substantial efforts to fix and utilize CO_2 through various strategies, problems remain for transforming CO_2 into other chemicals. Because of the highest oxidation state of the carbon atoms presented in CO_2, this process requires a large input of energy, resulting in more CO_2 emission on the basis of traditional energy sources (fossil fuels, etc.) and inevitably leading to additional pollution. Therefore, developing a reversible battery system for renewable energy storage in a CO_2 fixation way would be a double advantage idea, and Li-CO_2 batteries are exactly such devices using CO_2 as an energy carrier.[27]

1.4.1 Li-O_2/CO_2 Batteries

Since CO_2 can react with the active intermediate species $O_2^{\bullet-}$ or the discharge products to form carbonates in lithium-air batteries, it was originally taken as a contamination gas for the

main reaction between Li and O_2. Therefore, the Li-CO_2 batteries related research started from Li-O_2/CO_2 batteries, in order to understand the potential impact of CO_2 contamination.[5]

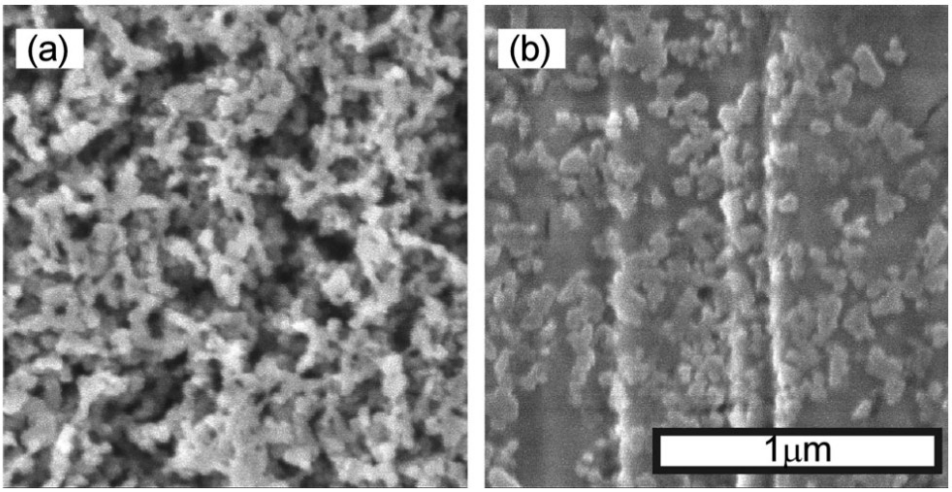

Fig. 1-17. Cross-section SEM images of the cathode of the Li-O_2/CO_2 battery (a) before and (b) after discharge (O_2:CO_2 = 1:1, current density: 0.1 mA/cm^2).[28]

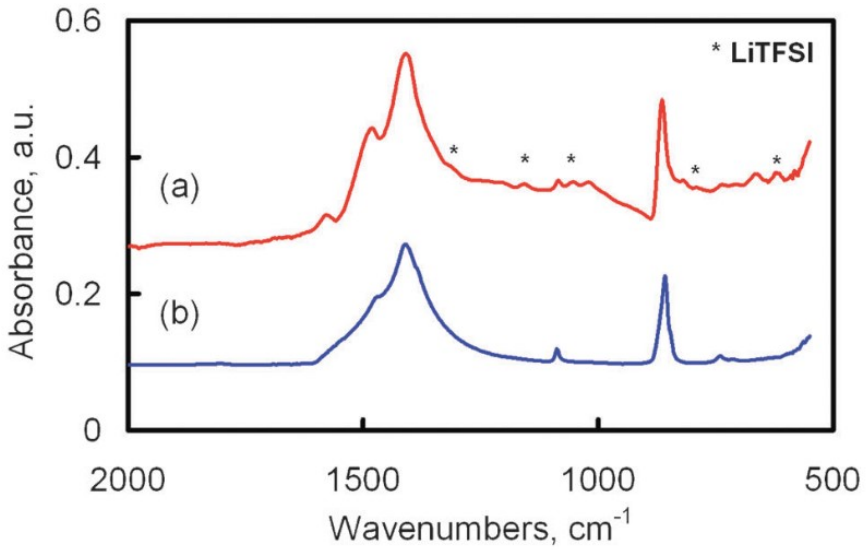

Fig. 1-18. IR Spectra of (a) the cathode of discharged Li-O_2/CO_2 battery and (b) standard Li_2CO_3.[28]

The primary Li-O_2/CO_2 battery was first reported by Takechi *et al*. in 2011.[28] Compared with

pure Li-O_2 batteries, Li-O_2/CO_2 batteries with a CO_2 ratio from 10-80% in the mixed gas showed higher discharge capacity, and no detectable amount of Li_2O_2 or Li_2O was found as discharge products. According to the SEM images (Fig. 1-17) and IR spectra (Fig. 1-18), only Li_2CO_3, whose morphology is quite different from that of Li_2O_2 or Li_2O, appeared on the surface of cathode after discharge. Moreover, the discharging plateau of Li-O_2/CO_2 batteries is about 2.7 V (Fig. 1-19), identical to that of Li-O_2 batteries. The mechanism of discharge processes of Li-O_2/CO_2 batteries were then proposed as following.

$$4O_2 + 4e^- \rightarrow 4O_2^{\cdot-}$$

$$O_2^{\cdot-} + CO_2 \rightarrow CO_4^{\cdot-}$$

$$CO_4^{\cdot-} + CO_2 \rightarrow C_2O_6^{\cdot-}$$

$$C_2O_6^{\cdot-} + O_2^{\cdot-} \rightarrow C_2O_6^{2-} + O_2$$

$$C_2O_6^{2-} + 2O_2^{\cdot-} + 4Li^+ \rightarrow 2Li_2CO_3 + 2O_2$$

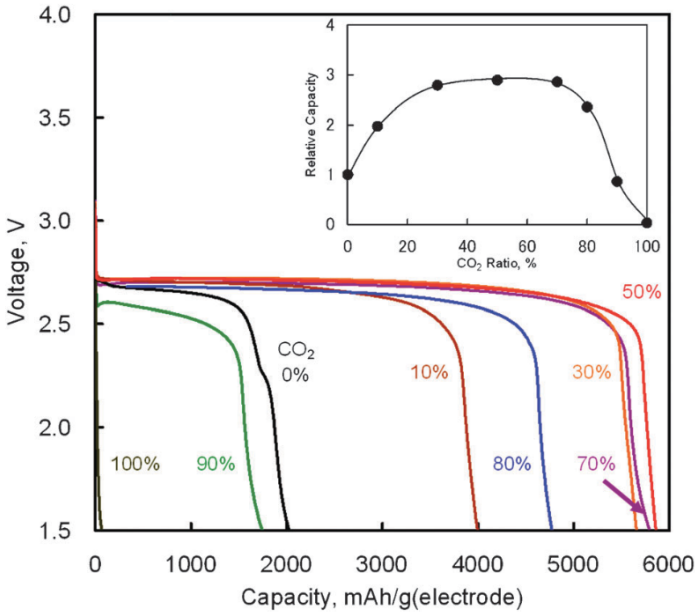

Fig. 1-19. Discharge curves of the Li-O_2/CO_2 batteries with various ratio of CO_2 in O_2/CO_2 mixed gas at 25 °C

(current density: 0.2 mA/cm^2).[28]

A new gas-utilizing battery with high discharge capacity was achieved in this work, for which the authors suggested that the key feature is the rapid consumption of superoxide anion radical by CO_2 as well as slow filling property of the final discharge product Li_2CO_3 in the cathode. However, a solution of 1 M lithium bis(trifluoromethanesulfonyl)imide (LiTFSI) in a mixture of ethylene carbonate (EC) and diethyl carbonate (DEC) (3:7 v/v), belonging to carbonate electrolytes, was used as an electrolyte in this article. Similar to the carbonaceous cathodes we discussed before, carbonate electrolytes are now known to undergo decomposition reactions in the discharge process of Li-O_2 batteries. Hence, such conclusions about Li-O_2/CO_2 batteries are impaired, and more efforts are needed to explore the real internal chemistry.

After that, CO_2 was considered as a complete contamination gas for rechargeable Li-O_2 batteries in several reports.[29,30] In Gowda *et al.*'s study[29], they discharged the assembled cells under three different atmospheres, pure CO_2, pure O_2, and a 10:90 CO_2/O_2 mixture (Fig. 1-20a). The cell discharged under pure CO_2 immediately failed, while the one discharged under a CO_2/O_2 mixture, which exhibited a larger discharge capacity, showed a similar discharge voltage plateau ($\sim$2.6 V) as the pure O_2 cell. Based on the above results, the authors suggested that no active Li-CO_2 electrochemistry was observed. Together with the significant Li_2CO_3 absorbance shown in Fourier transform infrared spectroscopy (FTIR) (Fig. 1-20b), it was postulated that the higher capacity of CO_2/O_2 cell resulted from changes of the deposit morphology where Li_2O_2 spontaneously reacted with CO_2 to form Li_2CO_3. Furthermore, CO_2 evolution from Li_2CO_3 during

battery charging was found to occur only at very high potentials (> 4 V) compared to O_2 evolution from Li_2O_2 (~3−3.5 V), and as a result, the presence of CO_2 during discharge drastically reduced the voltaic efficiency of the discharge-charge cycle (Fig. 1-20c). In order to understand the decomposition mechanism of Li_2CO_3, isotopic labeling measurements ($^{18}O_2$ and $C^{18}O_2$) were employed. However, O_2 isotopic scrambling was lacking during the charging process, indicating that the oxidation reaction cannot be the equation below.

$$Li_2CO_3 \rightarrow 2Li^+ + 2e^- + {}^1/_2\, O_2 + CO_2$$

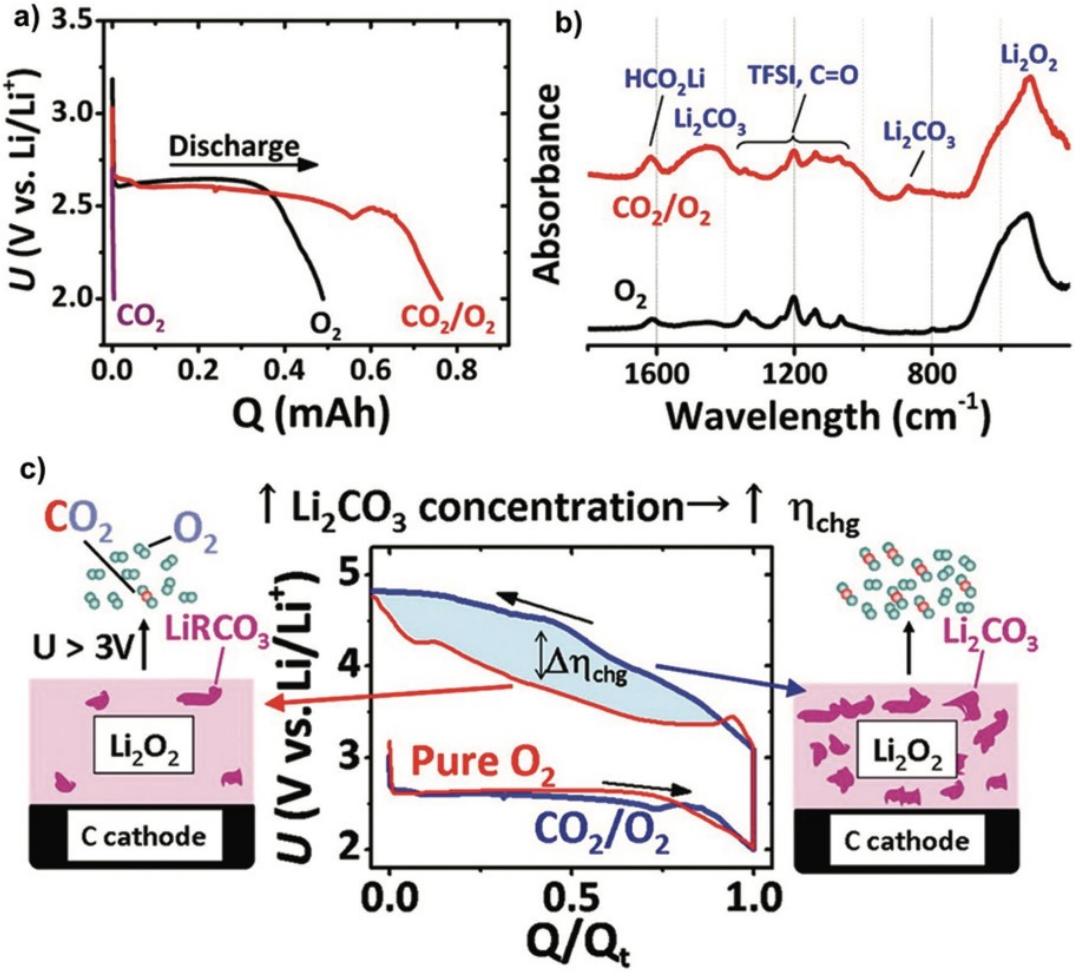

Fig. 1-20. (a) Galvanostatic discharge profiles (0.47 mA/cm^2) of Li cells discharged under pure CO_2, pure O_2, and

a 10:90 CO_2:O_2 mixture. XC72-based cathodes were used. (b) FTIR of cathodes extracted from cells discharged under pure O_2 and a 10:90 CO_2:O_2 mixture. (c) The voltaic efficiency of the discharge-charge cycle for cells under pure O_2 and a 10:90 CO_2:O_2 mixture.[29]

The electrochemical decomposition of Li_2CO_3 was finally ascribed to the mediation of electrolyte (i.e., dimethyl ether (DME) decomposed during and contributed to the CO_2 evolution reaction at high potentials), which could also result in the formation of DME-soluble decomposition products.[31]

In conclusion, the authors purposed to not only completely remove CO_2 from air fed to a rechargeable Li-air battery, but also to develop stable cathodes and electrolytes that will not decompose to form carbonate deposits during battery operation.

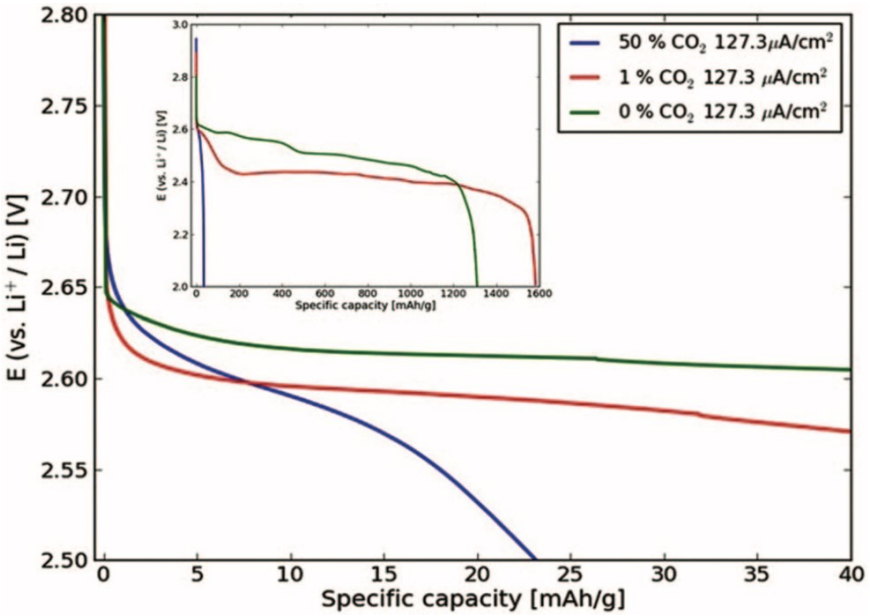

Fig. 1-21. Galvanostatic discharge profiles at 127.3 $\mu A/cm^2$ discharge at three different atmospheres: 50% CO_2, 1% CO_2, and 0% CO_2. Inset shows the increase in discharge capacity in 1% CO_2.[30]

The above conclusion was agreed by Mekonnen *et al*.[30] They studied the reactions between CO_2 and Li_2O_2 at the cathode by density functional theory (DFT) and galvanostatic charge-discharge measurements. From DFT computations, they suggested that CO_2 would block the surface-active nucleation sites and alter the shape and growth directions of Li_2O_2 on the surface with Li_2CO_3 formation. Meanwhile, their experimental results indicated that the charging processes were strongly influenced by CO_2 contamination, and exhibited increased overpotentials and increased capacity, which also resulted from poisoning of nucleation sites. This effect was experimentally observed even at 1% CO_2, and Larger capacity losses and overpotentials were seen at higher CO_2 concentrations (Fig. 1-21).

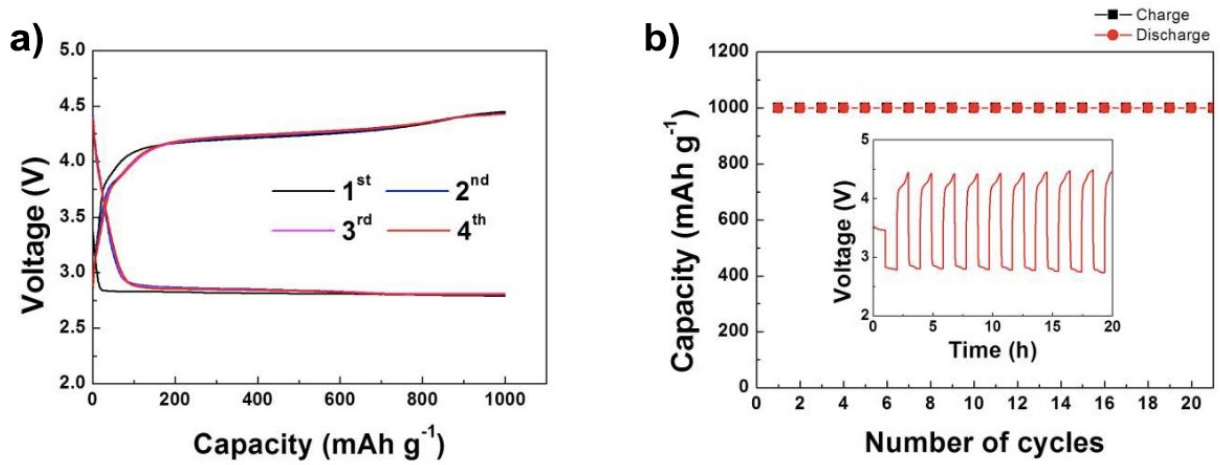

Fig. 1-22. (a) The initial 4 cycle profiles and (b) the related cyclability of the Li-O_2/CO_2 cell with DMSO electrolyte, utilized up to 1000 mAh/g at a constant rate of 0.4 mA/cm^2.[32]

Such frustrating results for Li-CO_2 electrochemistry were then explained by the Kang group after they investigated the reaction mechanisms in Li-O_2/CO_2 batteries under various electrolytes.[32] With quantum mechanical calculations and experimental verification, they found

that the subtle balance among various reaction pathways influencing the potential energy surfaces can be modified by the electrolyte solvation effect. In this way, a low dielectric electrolyte such as DME, consistent with former studies, tends to form Li_2O_2 as a primary discharge product, while a high dielectric electrolyte favors the reaction between the $O_2^{\bullet-}$ radical and CO_2, yielding only Li_2CO_3. Most surprisingly, they determined, for the first time, that the electrochemical activation of CO_2 within DMSO-based electrolyte enables the reversible formation of Li_2CO_3 instead of Li_2O_2, realizing a reversible Li-O_2/CO_2 (50% CO_2) battery which could run over 20 cycles with controlled capacity of 1000 mAh/g at 0.4 mA/cm^2 (Fig. 1-22).

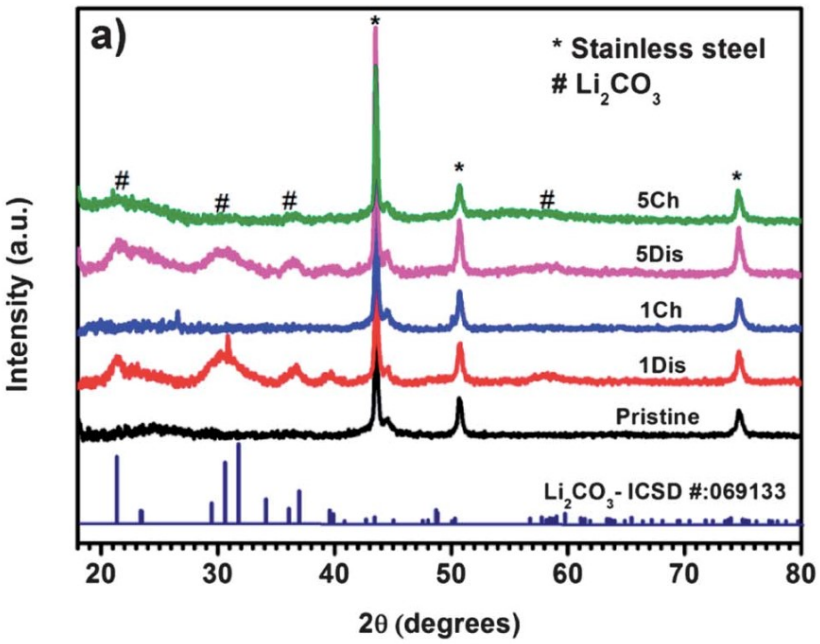

Fig. 1-23. The XRD pattern of Li-O_2/CO_2 battery (1:2 v/v), the first discharge, first charge, fifth discharge and fifth charge state.[35]

However, some reports[33,34] have revealed that sulfoxide is susceptible to nucleophilic attacks by reduced oxygen species, which calls on more attention paid to the chemical stability

of electrolytes. After that, Liu *et al.* reported a rechargeable Li-O_2/CO_2 battery (O_2:CO_2 = 1:2 v/v) with discharging specific capacity of 1808 mAh/g using lithium triflate ($LiCF_3SO_3$)-TEGDME as the electrolyte.[35] XRD patterns show that Li_2CO_3, which can be decomposed reversibly, is the main discharge product in the cell, and its reflections remain after the fifth charge (Fig. 1-23). This fact explains the rapid increase in overpotentials during the subsequent cycling.

Note that the electrochemical reduction of CO_2 is a key factor for the CO_2 utilization in battery systems. CO_2 does not participate in redox reactions among all the above Li-O_2/CO_2 batteries.

1.4.2 Primary Li-CO_2 Batteries

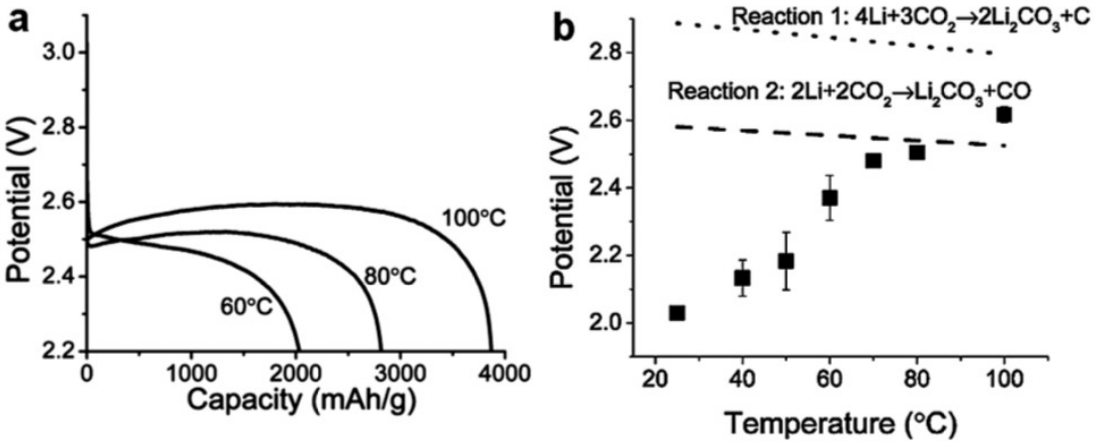

Fig. 1-24. (a) Galvanostatic discharge curves of Li-CO_2 cells operated at various temperatures in the range 60-100 °C at a current density of 0.05 mA/cm^2 to the potential of 2.2 V. (b) The comparison of theoretical equilibrium potential with actual discharge potential.[36]

The first Li-CO_2 battery with pure CO_2 as its cathode gas was reported by Xu *et al.* in 2013,[36] which was realized as a primary battery. The battery exhibits a high discharge capacity of ~2500

mAh/g at moderate temperatures, but the discharge capacity at 100 °C is nearly 1000% higher than that at 40 °C (Fig. 1-24a). The battery was equipped with a conductive carbon cathode and an ionic liquid electrolyte comprised of 1 M LiTFSI in the ionic liquid 1-butyl-3-methylimidazolium bis(trifluoromethanesulfonyl) imide ([bmim][Tf2N]). *Ex-situ* FTIR and XRD analyses convincingly show that Li_2CO_3 is the main component of the discharge product.

From combined experimental results and theoretical analysis of the solid products and the absence of CO in the gas products, the overall reaction was concluded as

$$4\mathrm{Li} + 3\mathrm{CO_2} \rightarrow 2\mathrm{Li_2CO_3} + \mathrm{C}$$

instead of the simplest known reaction between Li and CO_2 below.

$$2\mathrm{Li} + 2\mathrm{CO_2} \rightarrow \mathrm{Li_2CO_3} + \mathrm{CO}$$

It is evident in Fig. 1-24b that the measured cell potential initially approaches the calculated equilibrium potential, but then surpasses it. Based on Tafel theory, the actual discharge potential cannot exceed the theoretical equilibrium potential, so that the Reaction 2 is unlikely to dominate the discharge process. Nevertheless, the formation of carbon and the absence of CO was only deduced by an exothermic reaction that was not further investigated.

$$2\mathrm{CO} \rightarrow \mathrm{CO_2} + \mathrm{C}$$

After all, the produced carbon was hard to detect due to the application of carbon cathodes.

Their study showed that increasing the operation temperature could improve the Li_2CO_3 product accumulation on the carbon cathode as an insulating coating, which in turn promotes both the cell potential and discharge capacity.[37] Although the discharge capacity of Li-CO_2 batteries enormously rose with the operation temperature, the temperature dependence was

considerably weaker for cells based on carbon cathodes with high surface area. Therefore, a possible approach to realize room-temperature Li-CO_2 batteries was provided by exploring cathode materials with high surface areas and appropriate pore volumes.

1.4.3 Rechargeable Li-CO_2 Batteries

Due to the high decomposition potential of insulating Li_2CO_3, two pathways with different CO_2 electrochemistry, promoting Li_2CO_3 decomposition and producing other products with lower decomposition potentials, have been developed to realize rechargeable Li-CO_2 batteries.

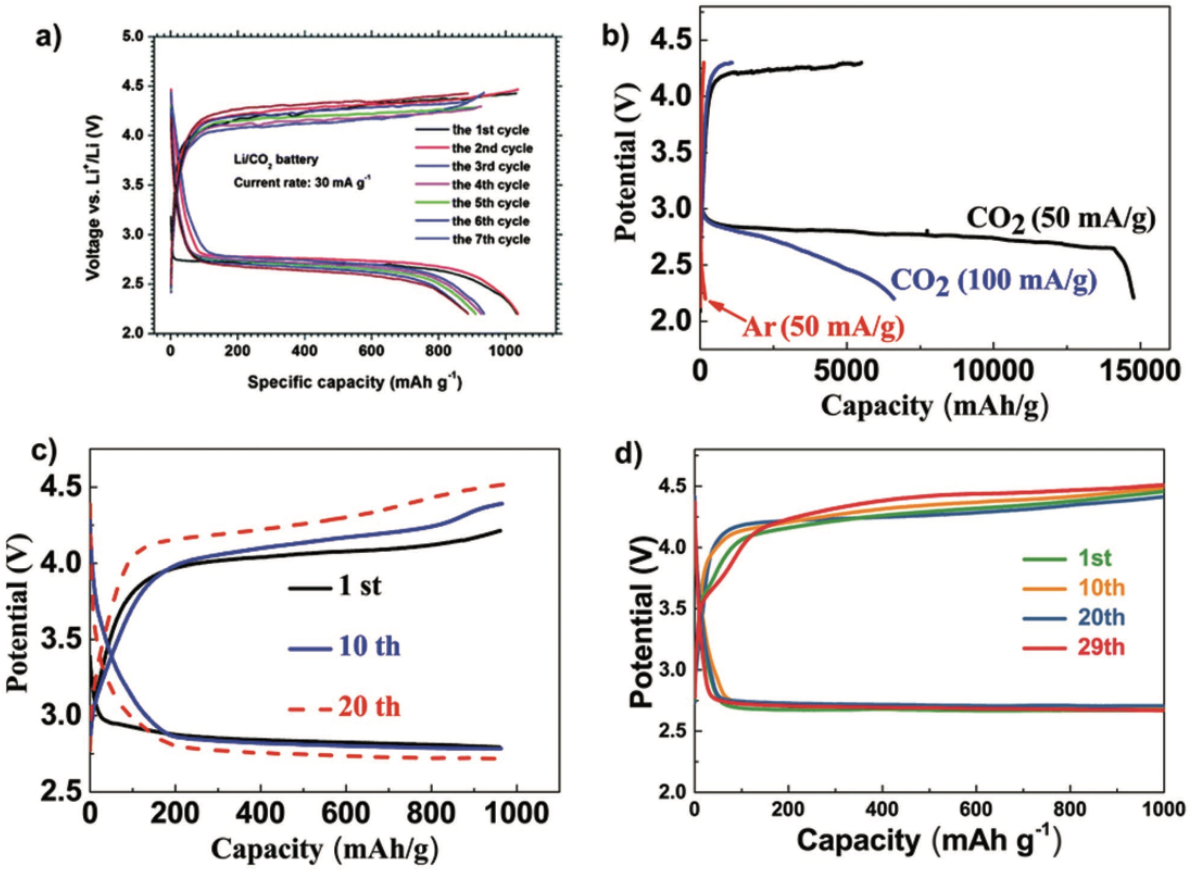

Fig. 1-25. (a) Charge-discharge profiles of Li-CO_2 batteries with the KB cathode under a cutoff voltage of 2.2 V at 30 mA/g.[35] (b) The initial discharge curves of the batteries with graphene cathodes in different atmospheres.

Cycling performance of Li-CO_2 batteries under a cutoff capacity of 1000 mAh/g at 50 mA/g with (c) graphene[39] and (d) CNTs cathodes.[41]

Since the rechargeable Li-CO_2 batteries are based on the same reaction as purposed for the primary Li-CO_2 battery,[36] plenty of catalyst cathodes with high surface area to accommodate solid products and electrocatalytic activity for Li_2CO_3 decomposition have been reported in recent years.

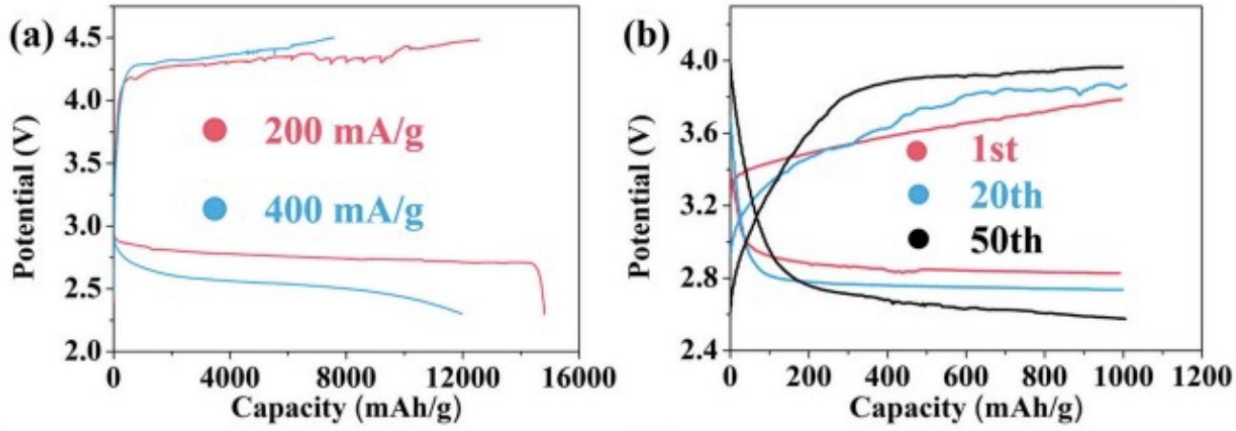

Fig. 1-26. (a) Charge-discharge profiles of Li-CO_2 batteries with the Cu-NG cathode at 200 and 400 mA/g. (b) Cycling performance under a cutoff capacity of 1000 mAh/g at 200 mA/g.[40]

Besides the Li-O_2/CO_2 battery, Liu *et al.* also realized a room-temperature Li-CO_2 battery with a normal Ketjen black (KB) cathode and a conventional electrolyte of $LiCF_3SO_3$ in TEGDME.[35] The Li-CO_2 cells could reversibly discharge and charge for 7 cycles with a cutoff capacity of 1000 mAh/g at 30 mA/g (Fig. 1-25b). When pursuing the utilization of transition metal carbonates as anode materials for Li-ion batteries, the Zhou group found that CO_2 can be probably utilized through electrochemical catalytic conversion reactions.[38] In addition, they introduced metal-free

graphene[39] and Cu dispersed nitrogen doped graphene[40] as air cathodes, as well as the carbon nanotubes (CNTs)[41]. A discharge capacity of 14774 mAh/g (Fig. 1-25b) and stable cyclability over 20 cycles (Fig. 1-25c) were achieved with metal-free graphene, while the cell with CNTs stably cycled for 29 cycles with controlled capacity of 1000 mAh/g at 50 mA/g (Fig. 1-25d). Li-CO_2 batteries with Cu dispersed nitrogen doped graphene cathodes achieved a discharge capacity of 14864 mAh/g at 200 mA/g (Fig. 1-26a) and ran over 50 cycles (Fig. 1-26b). They ascribed the higher electrochemical performance to the excellent electrical conductivity, large surface area, and high electrochemical stability of graphene and CNTs. Moreover, Li-CO_2 batteries with Ru/Ni foam cathodes have further increased the cycling performance to over 100 cycles with a charge voltage below 4.1 V (Fig. 1-27).[42]

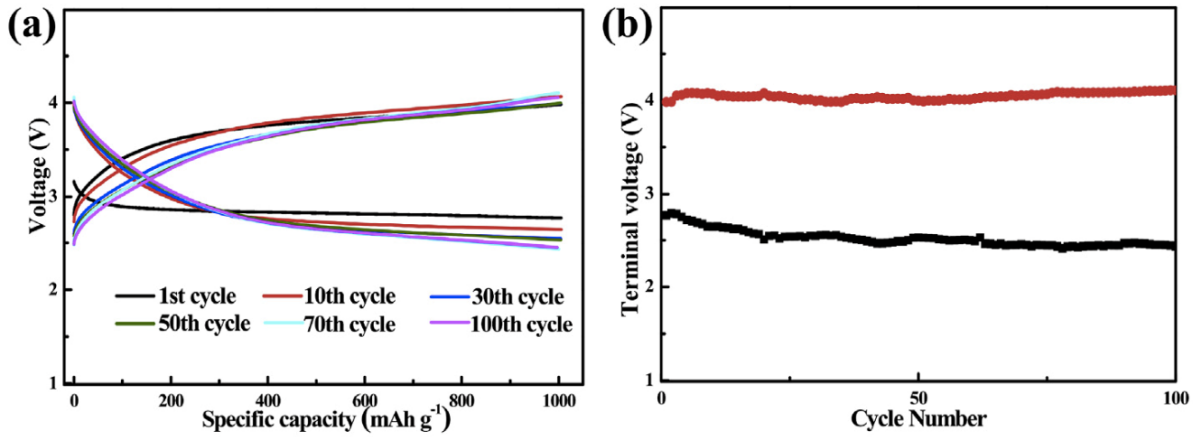

Fig. 1-27. (a) Discharge-charge profiles of the Li-CO_2 batteries with the Ru/Ni cathode at different cycles and (b) the corresponding voltages at the end of the discharge-charge process.[42]

In such Li-CO_2 electrochemical system, the reversible formation and decomposition of Li_2CO_3 has been confirmed by XRD and FTIR, which generates carbon product as well. Despite the

discussion remaining about how CO_2 is activated and further reacts, it is an appealing consensus that CO_2 in nonaqueous Li-CO_2 batteries reacts like in aprotic CO_2 electrolysis as following: one CO_2 molecule reacts with another after reduced to CO_2^- with one-electron transfer. The formed $C_2O_4^{2-}$ further reacts with CO_2, leading to finally C and Li_2CO_3 formation step by step.[6]

$$CO_2 + e^- \rightarrow {CO_2}^-$$

$${CO_2}^- + {CO_2}^- \rightarrow {C_2O_4}^{2-}$$

$${C_2O_4}^{2-} + CO_2 \rightarrow 2{CO_3}^{2-} + C$$

$$2{CO_3}^{2-} + 2Li^+ \rightarrow Li_2CO_3$$

The overall battery reaction of rechargeable Li-CO_2 batteries with Li_2CO_3 and C products can also be described as the equation below.

$$4Li + 3CO_2 \leftrightarrow 2Li_2CO_3 + C$$

Based on such a reaction, the theoretical voltage is about 2.8 V, which is roughly consistent with the experimental value.

On the other hand, oxalate was indicated to be formed in rechargeable Li-CO_2 batteries with a designed Mo_2C/CNT catalyst cathode, based on another mechanism.[43,44] In these batteries, generated $C_2O_4^{2-}$, the intermediate reduction product of CO_2, was stabilized by the Mo_2C catalyst rather than further reacted to form Li_2CO_3 and C, leading to a rechargeable Li-CO_2 battery with a charge voltage below 3.5 V. High energy efficiency (~80%) and improved cycling performance (40 cycles) were realized in such systems. Based on experimental results and the similar phenomenon of catalyst stabilization in the Li-O_2 battery, the possible reaction steps of Mo_2C for rechargeable Li-CO_2 battery were summarized in the following two equations and schematically

described in Fig. 1-28.

$$2CO_2 + 2e^- \rightarrow {C_2O_4}^{2-}$$

$${C_2O_4}^{2-} + 2Li^+ + Mo_2C \rightarrow Li_2C_2O_4 - Mo_2C$$

The first equation represents the one-electron reduction of CO_2 to $C_2O_4^{2-}$, the same process in Li_2CO_3 and C production. However, in the presence of Mo_2C, some metal-oxygen coupling between Mo in Mo_2C and O in C_2O_4 stabilizes this unstable $C_2O_4^{2-}$ through coordinative electron transfer.[45] This can prevent the formation of insulating Li_2CO_3 and thus easily release CO_2 and Li^+ through uncoupling of the Mo-O chemical bond during charge, reducing the charge potential below 3.5 V. The overall reaction can also be written as the widely known equation between Lithium metal and CO_2 at room temperature.

$$2Li + 2e^- + 2CO_2 \leftrightarrow Li_2C_2O_4$$

In summary, CO_2 electrochemistry in nonaqueous Li-CO_2 batteries demonstrated high operating voltage and capacity as well as moderate cyclability. The reaction pathways without proton assistance lead to limited products, including C, Li_2CO_3, CO and $Li_2C_2O_4$. Although the reported Li-CO_2 batteries were tested only at low current density and with high overpotential, the rechargeable room-temperature Li-CO_2 battery is undoubtedly a novel CO_2 capture way as well as a promising energy storage system.

In spite of all these achievements of Li-CO_2 batteries, a thorough understanding of the electrochemical reaction of Li_2CO_3 has not been obtained. In addition to CO_2 gas, there are trace amounts of carbonates and carboxylates resulting from the degradation of the electrolyte and carbon cathode surface. In order to develop both CO_2 fixation techniques and Li-CO_2 batteries, a

comprehensive understanding of the reaction mechanism for CO_2 reduction and the subsequent oxidation process becomes crucial.

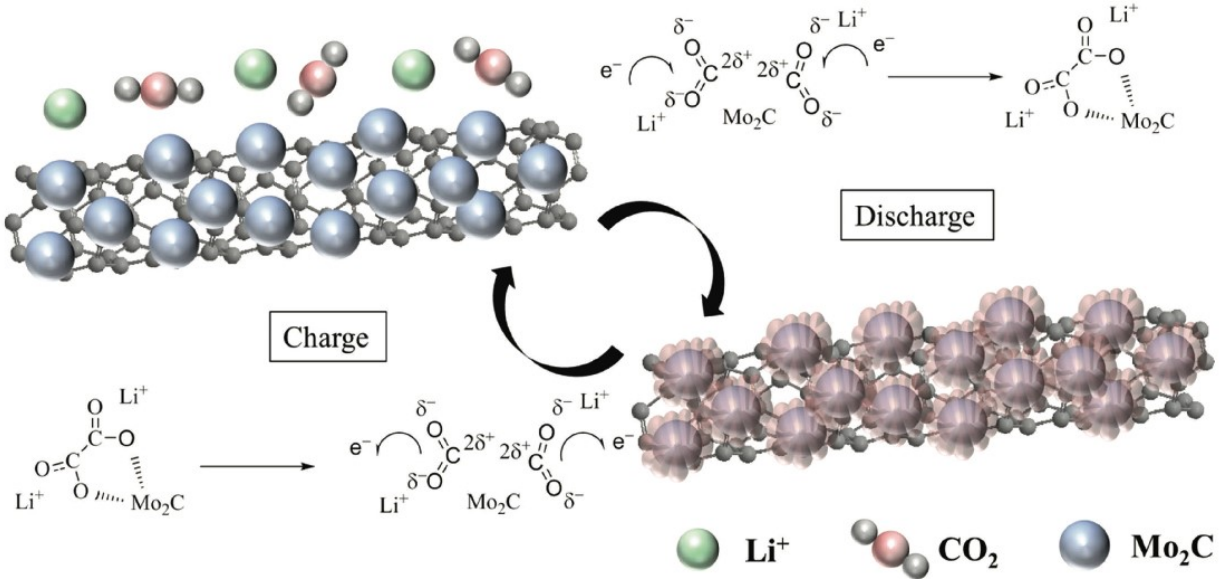

Fig. 1-28. Schematic illustration of reactions during discharge and charge of Mo_2C/CNT in the Li-CO_2 battery. CO_2 is reduced at the Mo_2C/CNT electrode surface on discharge, forming $Li_2C_2O_4$, and then this intermediate product is stabilized by Mo_2C, forming an amorphous discharge product that can be easily decomposed on charge.[43]

1.5 Motivation

The purpose of this work is to develop lithium-gas battery systems based on the molten salt Li-O_2 battery, employing novel inorganic electrolytes and noncarbonaceous cathodes at high operation temperature. We expect more possibilities by expanding this electrochemical system from O_2 to other reactive gases, such as CO_2.

In this way, we can realize and explore some electrocatalytic reactions, such as oxygen

reduction reactions (ORR), oxygen evolution reactions (OER), CO_2 reduction and evolution reactions, in the battery systems. Without the disturbances from organic electrolytes and carbonaceous cathodes, the products detection will provide more convincing evidences to identify the reaction mechanism. In addition, the improved kinetics brought by high temperature is also a desired factor for such gas reactions. All these advantages make the molten salt lithium-gas battery an attractive catalytic system besides an energy storage device.

This thesis presents two Li-gas electrochemical systems, Li-O_2 batteries and Li-CO_2 batteries. The preparation of required battery components was illustrated, including the nickel-nitrate composite cathode, carbon-nitrate composite cathode, separators (nitrites soaked glass fiber and LAGP solid electrolyte membrane). We evaluated the electrochemical performances of the batteries through charge-discharge cycling under different conditions and cyclic voltammetry (CV). To confirm the products during charge-discharge process, we carried out X-ray diffraction (XRD) to identify solid compositions, while *in-situ* gas chromatography-mass spectrometry (GC-MS) was employed to measure gas products.

2 Experimental Section

2.1 Battery Components Preparation

The configurations of the investigated Li-O_2 and Li-CO_2 batteries are similar, which refer to the setup reported earlier by Xia *et al*.[23]

2.1.1 $LiNO_3$-KNO_3 Molten Salt Electrolyte

Since the melting point of lithium metal is 180.50 °C,[46] the operation temperature should not above this number in order to maintain the Li anode in solid phase. However, the melting point of the effective composition in inorganic electrolytes, lithium nitrate ($LiNO_3$), is 254.5°C,[47] which means other components are needed to form a eutectic system with $LiNO_3$, lowering the liquidus temperature of the molten salt electrolyte. It was found by Giordani *et al.*[7] that $LiNO_3$-KNO_3 mixture is currently one of the most suitable Li^+-bearing electrolytes known for the reversible oxygen electrochemistry occurring in the Li-O_2 battery, which was also employed by Xia *et al*.[23] later. Compared with another electrolyte purposed by Giordani *et al.*[7], $LiNO_3$-KNO_2-$CsNO_3$, the binary system $LiNO_3$-KNO_3 is easier to control. More importantly, the eutectic point of $LiNO_3$-KNO_3 (~125 °C) is higher than that of $LiNO_3$-KNO_2-$CsNO_3$ (~90 °C), and the relatively high temperature is essential for catalytic reactions. Therefore, $LiNO_3$-KNO_3 mixture was used as the electrolyte for both Li-O_2 and Li-CO_2 batteries in our work.

Lithium nitrate ($LiNO_3$) and potassium nitrate (KNO_3) were purchased from Sigma-Aldrich. The mole ratio of $LiNO_3$/KNO_3 is 42:58 when preparing the molten nitrate salt electrolyte, which corresponds to the composition at the eutectic point in the $LiNO_3$-KNO_3 phase diagram (Fig. 2-1).

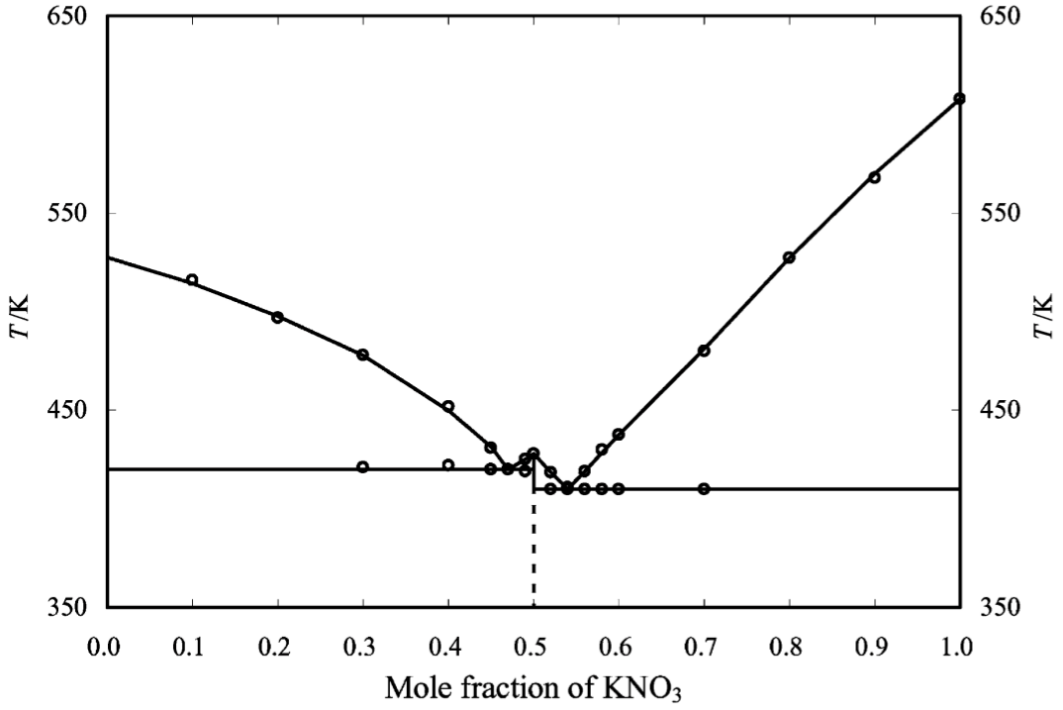

Fig. 2-1. The phase diagram for the $LiNO_3$-KNO_3 system.[47]

To ensure the glass fiber separators (Whatman) were fully and uniformly wet by the nitrates mixture, instead of using $LiNO_3$-KNO_3 molten salt, the electrolyte soaked separators were prepared by immersing the glass fiber paper in an aqueous solution of $LiNO_3$-KNO_3 (mole ratio of 42:58) at a salt concentration of 0.25 g/mL. The wetted glass fiber discs were placed in a 180 °C oven for 20 min to evaporate water and allow the absorbed nitrates to melt, forming a molten salt. This process was repeated three times until all of the pores in the glass fiber were filled. After that, the electrolyte-filled separators were transferred to an Erlenmeyer flask (Synthware) placed in oil bath, and vacuum-dried at 200 °C for one day, before they were put into the glovebox for cell assembly.

2.1.2 $Li_{1.5}Al_{0.5}Ge_{1.5}(PO_4)_3$ (LAGP) Solid Electrolyte Membrane

$Li_{1.5}Al_{0.5}Ge_{1.5}(PO_4)_3$ (LAGP) solid electrolyte membranes were prepared with commercial LAGP powder purchased from MSE Supplies. For each membrane disc, 500 mg solid electrolyte powder was pressed with 10 tons of pressure for 30 sec. The resulting white discs were sintered at 900 °C for 10 hrs at programmed heating and cooling ramp rates of 1 °C/min. The morphology of LAGP discs was detected by SEM and shown in Fig. 2-2. The SEM images indicate a good crystallization as all grains are connected to each other, which is the foundation for efficient Li-ions migration.

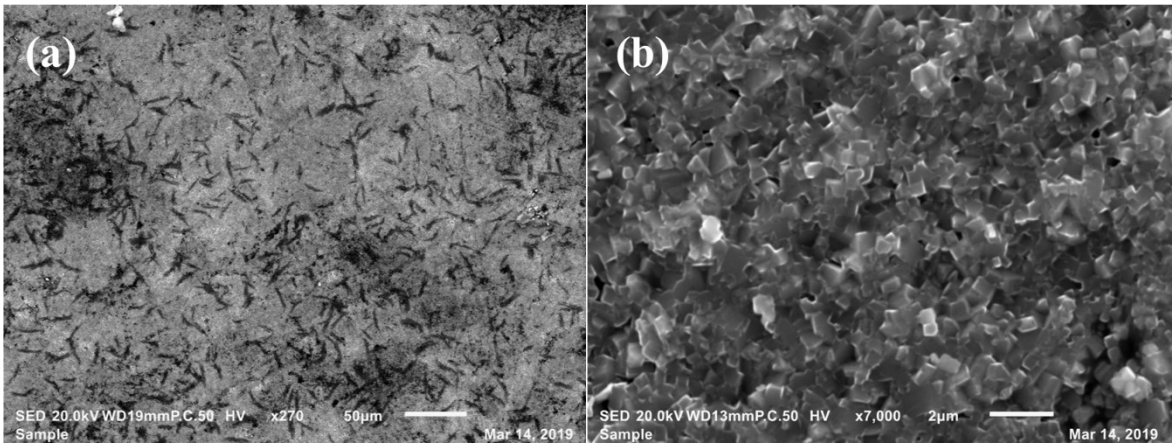

Fig. 2-2. (a) Top down and (b) cross-section SEM images of LAGP discs.

It is suggested that the reaction between Li and $LiNO_3$ will lead to the formation of Li_2O and $LiNO_2$ on the surface of lithium anode, which are soluble in the molten nitrate electrolyte, as described in the first equation below. Furthermore, the generated Li_2O and $LiNO_2$ may then react with the carbon cathode to form Li_2CO_3 (the second and third equations). As the analysis results shown in Fig. 2-3, LAGP can effectively reduce the crossover of these soluble by-products, reducing the undesired side reactions.[23]

$$2\mathrm{Li} + \mathrm{LiNO_3} \rightarrow \mathrm{Li_2O} + \mathrm{LiNO_2}$$

$$\mathrm{Li_2O} + \mathrm{C} + \mathrm{O_2} \rightarrow \mathrm{Li_2CO_3}$$

$$\mathrm{Li_2O} + \mathrm{C} + 2\mathrm{LiNO_3} \rightarrow \mathrm{Li_2CO_3} + 2\mathrm{LiNO_2}$$

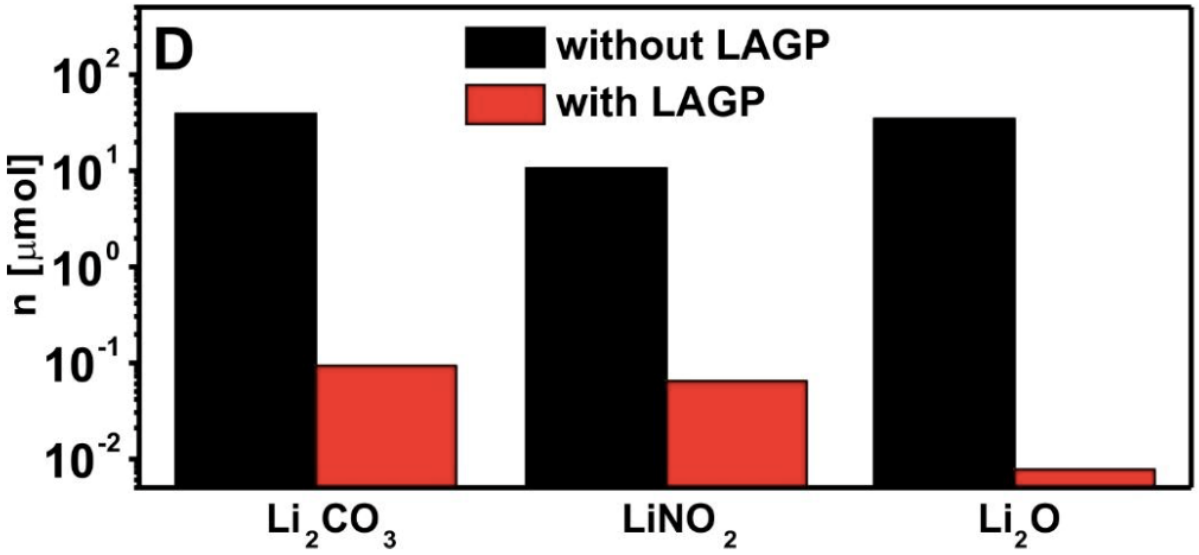

Fig. 2-3. Comparison of cathodic products in the absence (black) and presence (red) of the LAGP solid electrolyte at OCV after 64 hrs.[23]

2.1.3 Ni-nitrate Composite Cathode

Typically, 40 mg Ni nanopowder (Sigma-Aldrich) was mixed with 4 mL $LiNO_3$-KNO_3 aqueous solution (0.25 g/mL) by ultrasonic. The mixture was then dripped to stainless steel mesh current collectors with 200μL on each piece. After that, the stainless steel mesh discs were heated in an oven at 180 °C for one day prior to use, in order to remove water and to form a thin layer of molten nitrate on the Ni nanoparticles.

2.1.4 Carbon-nitrate Composite Cathode

To compare with the Ni-nitrate composite cathode, commonly-used carbon cathode was

prepared in a similar way and tested in molten salt Li-O_2 batteries. The carbon cathode was composed of 85% Super P carbon (MTI Corporation) and 15% PTFE (Alfa Aesar), which were mixed and dispersed in N-Methyl-2-Pyrrolidone (NMP). About 5 mg carbon materials from the mixture and 25 mg salts from $LiNO_3$-KNO_3 aqueous solution were dripped onto each stainless steel mesh, resulting in a carbon-nitrate composite cathode. The wet cathodes were then vacuum dried at 200 °C for one day before transferred to the glovebox.

2.2 Batteries Configuration and Assembly

A test cell for lithium-air battery (MTI Corporation) was employed for the electrochemical tests of Li-O_2 and Li-CO_2 batteries, which is shown in Fig. 2-4.

Fig. 2-4. The test cell used for Li-O_2 and Li-CO_2 batteries.

The Li-O_2 cell was assembled as depicted in Fig. 1-12b in an Ar gas filled glovebox. The anode was prepared by pressing lithium metal disc onto the stainless steel current collector, and was

placed at the bottom of battery. The dried glass fiber disc and LAGP membrane were then put into the battery one after another as separators. After that, the prepared Ni-nitrate composite cathode was placed on the top. Grinded $LiNO_3$-KNO_3 powder was sprinkled between each layer, making sure the battery body was filled with molten salt electrolyte when operated at high temperature. Before combining the upper half battery case with the base, these battery components were heated in an oven at 150 °C for 1 hr. When the nitrate mixture was in molten salt state, we pressed all the layers together for a better ions migration inside the battery.

After cooling down the assembled cell and taking it out of the glovebox, we constantly flowed through the cell with O_2 gas for 5 min to remove any atmospheric contamination as well as to completely fill the cathode area with O_2. We then turned off the valve to block O_2 gas and put the cell into an oven at 150 °C.

The assembly of Li-CO_2 cells was exactly same as Li-O_2 cells, except the cathode was filled with CO_2 (or the mixture of CO_2 and Ar) instead of O_2.

2.3 Electrochemical Tests

All the electrochemical tests for Li-O_2 and Li-CO_2 batteries were conducted at 150 °C, which is an ideal operation temperature for $LiNO_3$-KNO_3 molten salt electrolyte. The cells were connected to electrochemical test equipment at the same time when put into the oven after filled with the cathode gases.

2.3.1 Charge-Discharge Cycling

The charge and discharge processes of the Li-gas batteries were realized using a laboratory

battery tester from Arbin. The cells were galvanostatically cycled at different current densities, as well as cycled under a curtailing capacity. The cells were also discharged to various cutoff voltages to measure the products generated during different stages, determining the reaction mechanism of these batteries. All the assembled batteries were rested at 150 °C for 8 hrs before the measurement.

2.3.2 Cyclic Voltammetry (CV)

A cyclic voltammetry (CV) was performed to monitor the electrochemical processes of the batteries during cycling, as the presence of intermediates and the reversibility of reactions can be told from CV curves. The CV analysis was finished by AutoLab 302 potentiostat (Metrohm) electrochemistry testing station.

2.4 Materials Characterization

2.4.1 X-ray diffraction (XRD)

As a simple and fast characterization method for crystals, XRD was used to identify the solid products generated during charge and discharge processes. The XRD samples were prepared in the glovebox to prevent them from contamination or oxidation. After put on the quartz discs, the samples were sealed with Kapton tape.

2.4.2 Gas Chromatography-Mass Spectrometry (GC-MS)

The measurement of gas products generated during cycling is a tough problem due to the small amount of products, transfer issues, leakage concerns, and high operation temperature. GC-MS is an appropriate approach to identify the gas products as well as to determine their

concentrations. However, considering the typical procedure of *ex-situ* test, there is no protocol for how to collect the gas after reaction from the battery and inject it into GC-MS then. At first, we used a microsyringe to draw the gas from cathode and transfer it to the GC-MS QP2010SE instrument (Shimadzu) immediately after collection, but it was nearly impossible to stop air from blowing into the cathode once the valve was on.

Therefore, we developed an *in-situ* method to monitor the gas products at the same time of battery operation. Two pipes, the intake pipe and the outlet pipe, were linked to valves on the battery under cycling in 150 °C oven, directly connecting the battery with gas cylinders and GC-MS. In this way, the cathode gas from gas cylinders continuously flowed into the battery for reactions, and the generated gas products then flowed into the GC-MS for measurement. To prevent the molten salt electrolyte from solidification, the pipe between gas cylinder and battery was wrapped with an electric heating belt, making sure the gas flowing into the battery was at operation temperature.

The *in-situ* GC-MS measurement of gas products from Li-CO_2 batteries was performed following a specific protocol. Prior to the measurement, we first run GC-MS for the pre-mixed CO_2 (1200 ppm)/air gas at 2 SCCM to ensure the stability of CO_2 signal. The calibration curve was then drawn by mixing CO_2 with Ar at different ratios with a total gas flow of 10 SCCM. To analyze the discharge process, the CO_2-Ar gas mixed at a calculated ratio was purged into the battery. After that, the Li-CO_2 battery was discharged at 150 °C while GC-MS was simultaneously measuring the consumption of CO_2 and the formation of other gas products. For the charge process, the assembled battery was first filled with CO_2. Once the battery was discharged to the

lower voltage limit, pure Ar gas was purged into the battery to blow away all the CO_2 and other gases left. The battery was then connected to GC-MS with Ar gas blowing, and charged to the higher voltage limit to detect the reactions happening during this process.

3 Results and Discussion

3.1 Li-O_2 Batteries

3.1.1 Charge and Discharge Cycling

The stability of molten salt electrolyte Li-O_2 battery suggested in Xia's work[23] was tested through charge-discharge cycling. According to the literature, the initial amount of cathode material, Ni nanoparticles, we put on each stainless steel mesh was 200 mg, and the specific capacity was represented by the capacity per surface area. However, though the cell exhibits satisfactory cycling performance as shown in Fig. 3-1a, which is with good reproducibility, charge/discharge plateaus like those in Fig. 1-14a are not clearly observed. This means the resulted capacity cannot be definitely ascribed to the reactions between Li and O_2. In addition, the mass specific capacity is quite low (7.5 mAh/g) at such high loading of Ni.

We then reduced the amount of Ni on each mesh to 2 mg as described in the cathode preparation, and evaluated the performance by mass specific capacity. Significant plateaus appear in the charge-discharge profile (Fig. 3-1b), which accord with the results in the literature (Fig. 3-1c). More importantly, the mass specific capacity rises dramatically at an even higher current density. As no binder was used for the cathode, the combination of Ni nanopowder and stainless steel current collector was based on the electrostatic between them. Thus, for the batteries with high cathode loading, some Ni nanopowder may fall from the stainless steel mesh during cycling due to the weak binding force, leading to a low specific capacity calculated from the original mass. However, the voltage gap (~0.6 V) demonstrated in Fig. 3-1b is still larger than that in Fig. 3-1c (red solid curve), which may be related to the catalytic effects disparity resulted

from different preparation methods of the Ni-nitrate composite cathode.

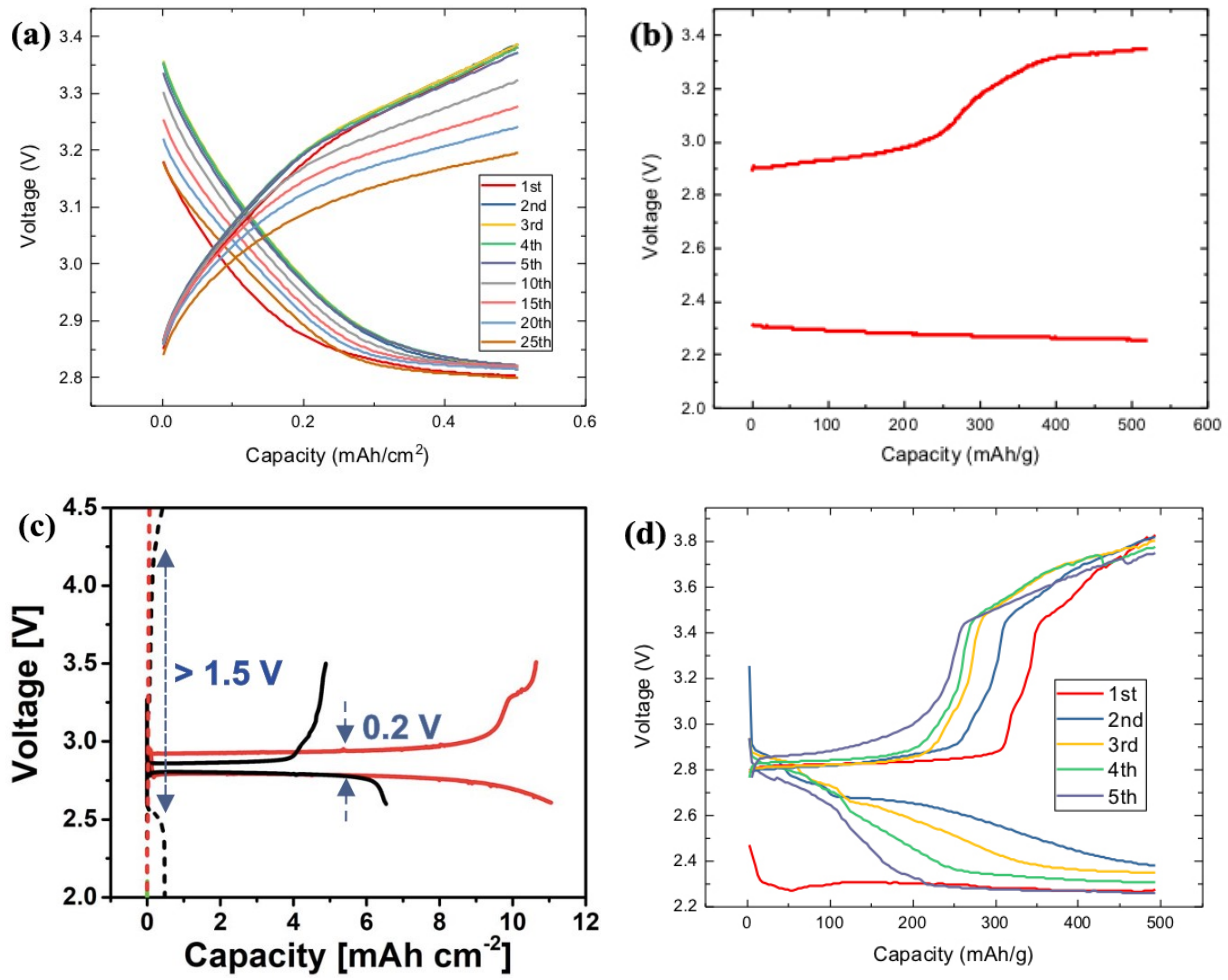

Fig. 3-1. Charge-discharge profiles of molten salt Li-O_2 batteries employing the Ni-nitrate composite cathode (a) with 200 mg Ni loading at 4 mA/g. (b) with 2 mg Ni loading at 80 mA/g. The cutoff capacity is 500 mAh/g. (c) First discharge and charge curves of Li-O_2 cells in Xia's work with a carbon cathode (black) and a Ni-based cathode (red). The cells using aprotic electrolyte (0.5 M LiTFSI in TEGDME) were examined at 25°C (dashed lines), whereas the cells using the molten nitrate electrolyte were measured at 150°C (solid lines). The current density is 0.1 mA/cm^2, and voltage window is 2.6-3.5 V.[23] (d) Charge-discharge profiles of molten salt Li-O_2 batteries with the carbon cathode with 5 mg carbon loading under the cutoff capacity of 500 mAh/g at 80 mA/g.

In contrast, the cycling stability of the molten sat Li-O_2 battery with carbon cathode is not so satisfactory, in spite of the moderate capacity and voltage gap (Fig. 3-1d). A number of plateaus are observed in charge and discharge curves, corresponding to different voltages at various cycle numbers. This may indicate the complicated side reactions happening in the Li-O_2 battery, which are caused by the utilization of carbon cathode.

Thus, the feasibility of molten salt Li-O_2 battery using $LiNO_3$-KNO_3 mixture and Ni-nitrate composite cathode has been confirmed. After modifying the preparation protocol according to the electrochemical performance, it showed stable cycling performance, reasonable capacity, moderate voltage gap, as well as clear charge/discharge plateaus. In this way, we then applied the molten salt electrolyte to Li-O_2 batteries to not only develop a new energy storage system, but also explore the mechanism of CO_2 conversion.

3.2 Li-CO_2 Batteries

3.2.1 Charge and Discharge Cycling

The Li-CO_2 batteries were assembled in the same way as Li-O_2 batteries, and cycled at current densities of 50 mA/g (Fig. 3-2a), 75 mA/g (Fig. 3-2b) and 100 mA/g (Fig. 3-2c). The cycling was limited by the cutoff capacity of 500 mAh/g and the cutoff voltages of 1.5 V and 5.0 V. Fig 3-2b,c clearly show that the capacity increases first before fading, and the maximum capacity appears at the 4^{th} or 5^{th} cycle. This phenomenon can also be observed in some lithium ion batteries. As batteries using certain materials may have not been fully activated before the first cycle, it will take several cycles to completely exhibit the capacity. Fig. 3-2c shows that the molten

salt electrolyte Li-CO_2 batteries can successfully run more than 30 cycles at a relatively large current density. The maximum discharge capacity at the 4th cycle is 463 mAh/g, while the capacity retention rate remains 83.8% after 30 cycles. The charge curve in Fig. 3-2a reveals two obvious plateaus at ~3.4 V and ~4.0 V, which correspond to the CV result (Fig. 3-4) shown in later section. Fig. 3-2d compares first discharge and charge curves of the Li-CO_2 cells at different current densities. The charge/discharge curve at 50 mA/g shows a small voltage gap of ~0.6 V, which increases with the current density, and the first charge plateau at ~3.4 V also becomes not so significant at large current density.

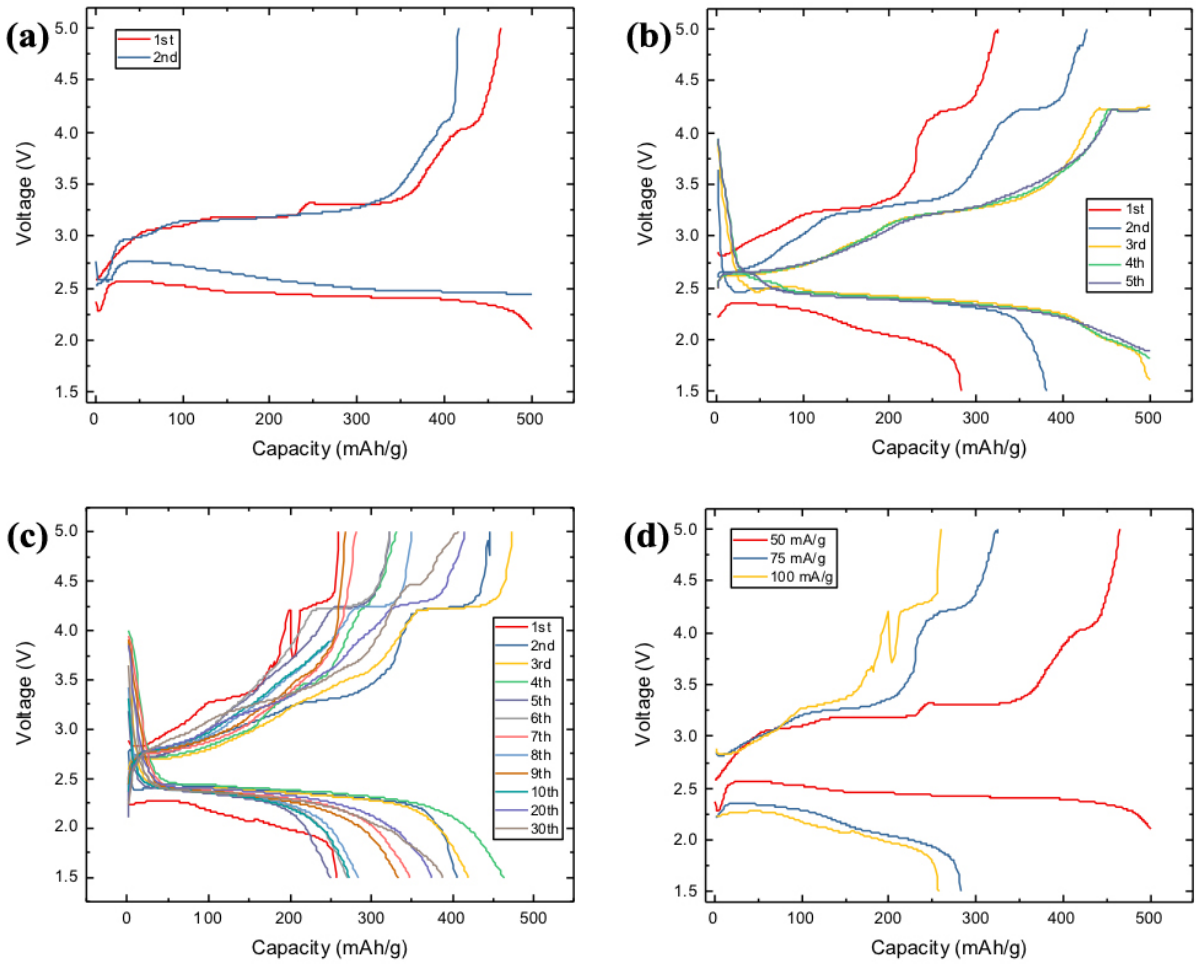

Fig. 3-2. Charge-discharge profiles of molten salt Li-CO_2 batteries with the Ni-nitrate composite cathode at the current density of (a) 50 mA/g, (b) 75 mA/g, (c) 100 mA/g. (d) First discharge and charge curves of Li-CO_2 cells at different current densities of 50 mA/g, 75 mA/g and 100 mA/g. The cutoff capacity is 500 mAh/g and the voltage window is 1.5-5.0 V.

When compared with the first charge-discharge curve of the Li-O_2 cell, the Li-CO_2 cell demonstrates different charge/discharge voltages as well as plateaus, which indicates that the reaction mechanism of these two kinds of Li-gas batteries are different despite the identical assembly and measurement.

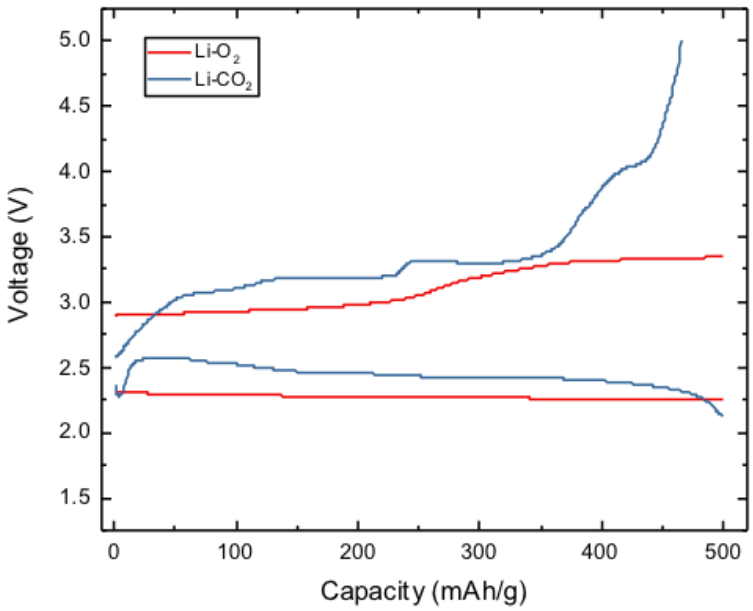

Fig. 3-3. First discharge and charge curves of the Li-O_2 battery at 80 mA/g (red curve) and the Li-CO_2 battery at 50 mA/g (blue curve) under the cutoff capacity of 500 mAh/g.

Based on above cycling results, it has been proved that the molten salt electrolyte and Ni-nitrate composite cathode can be well applied to Li-CO_2 batteries, showing good cycling

performance and satisfactory specific capacity. The stable charge/discharge curves with significant plateaus can be convincing evidences to identify the mechanism of Li-CO_2 batteries operated under such untypical conditions.

3.2.2 Cyclic Voltammetry (CV)

Fig. 3-4 exhibits the CV curves of the molten salt electrolyte Li-CO_2 batteries with Ni-nitrate composite cathode between 2.5 and 4.2 V at a scan rate of 5 mV/s. Two obvious anodic peaks at ~3.6 V and ~4.0 V can be observed, which should correspond to the oxidation of amorphous products like $Li_2C_2O_4$-based intermediate (the first equation below) as well as the decomposition of carbon and Li_2CO_3 (the second equation) according to the previous reports.[42,43,48]

$$Li_2C_2O_4 \rightarrow 2Li + 2e^- + 2CO_2$$

$$2Li_2CO_3 + C \rightarrow 3CO_2 + 4Li^+ + 4e^-$$

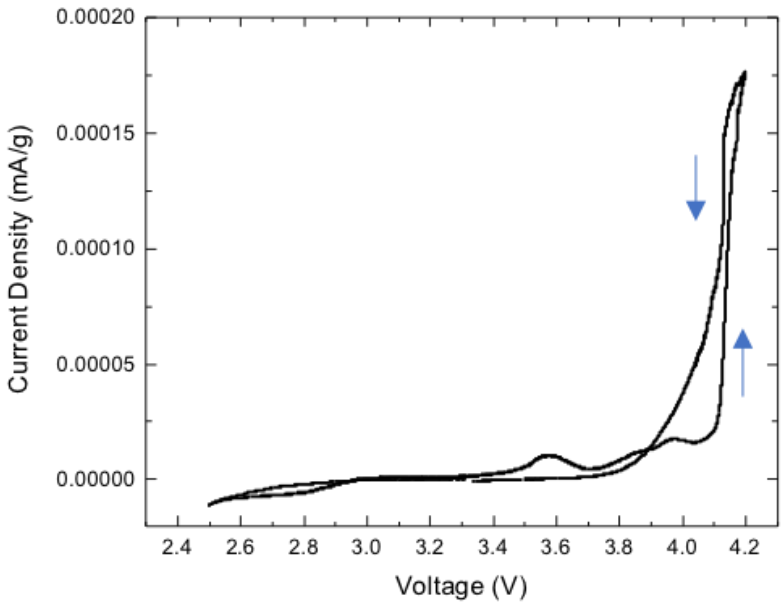

Fig. 3-4. CV curves of the molten salt electrolyte Li-CO_2 cell with a scan rate of 5 mV/s.

In addition, these anodic peaks match the discharge plateaus shown in the cycling curves in Fig. 3-2a, which further confirms the purposed reaction mechanism of Li-CO_2 batteries. Though not so apparent the cathodic peak is, it should be related to the CO_2 reduction reaction during discharge.

3.2.3 X-Ray Diffraction (XRD)

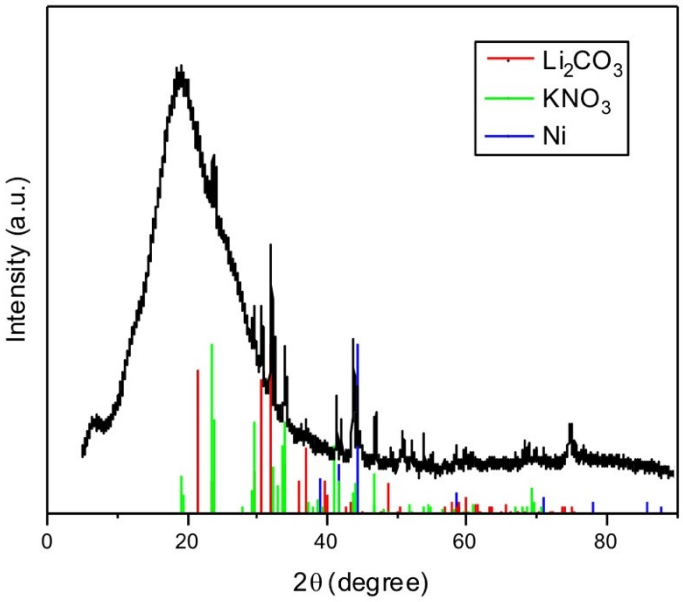

Fig. 3-5. XRD pattern of the Ni-nitrate composite cathode discharged to 1.5 V. Reference patterns of Li_2CO_3 (#22-1141) KNO_3 (#05-0377) and Ni (#45-1027).

The solid discharge products were characterized by XRD after the discharged Li-CO_2 cell was disassembled and the sample was prepared in the Ar filled glovebox. Besides the Ni cathode material and KNO_3 in the molten salt electrolyte, the discharged cathode also showed reflections of Li_2CO_3, which is the discharge product of Li-CO_2 batteries according to the purposed mechanism. Since inorganic electrolyte and noncarbonaceous cathode were employed, there

should be no other carbon source except CO_2. In other words, Li-CO_2 batteries using molten salt electrolyte and Ni-nitrate composite cathode confirm Li_2CO_3 to be the discharge product in a more persuasive way than those with conventional organic electrolyte and carbon cathode. For another suggested discharge product, carbon, its reflections was not observed in the XRD pattern due to the typical amorphous form. Therefore, the formation of carbon on the discharged cathode needs to be verified through characterization methods other than XRD.

3.2.4 Gas Chromatography-Mass Spectrometry (GC-MS)

It was initially expected to observe the concentration change of certain gases in the working Li-CO_2 cell during discharge and charge processes by *in-situ* GC-MS, so that the reaction between Li and CO_2 can be inferred from the consumption of CO_2 and the generation of other gas products. Before testing, the calibration curve (Fig. 3-6) was first acquired by measuring a series of CO_2-Ar mixture gas with different ratios.

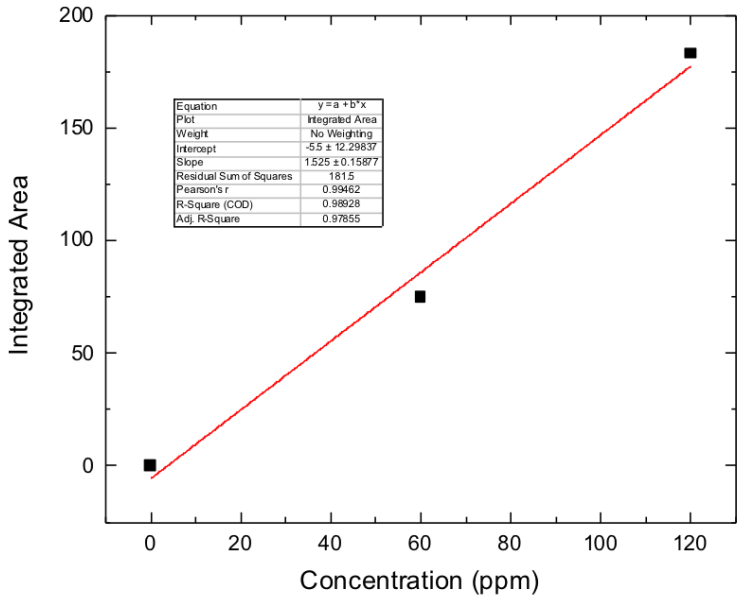

Fig. 3-6. The calibration curve of CO_2 concentration measured by GC-MS.

During cycling, H_2 was detected by *in-situ* GC-MS (Fig. 3-7c), and thus we measured empty battery case and assembled Li-CO_2 cell without cycling at 150 °C to confirm the source of H_2. As shown in Fig. 3-7a,b and summarized in Table 3-1, considering impurities and noises, H_2 should be generated from other components in the assembled battery instead of a gas product from charge/discharge reactions. Moreover, CO was not significantly detected by *in-situ* GC-MS in all three situations.

Table 3-1. Existence of CO and H_2 in empty battery case, molten salt Li-CO_2 cell without and during cycling

composition	empty battery case	molten salt Li-CO_2 cell without cycling	molten salt Li-CO_2 cell during cycling
CO	×	×	×
H_2	×	√	√

However, when we tried to monitor the consumption and generation of CO_2 during discharge and charge processes, we found it was hard to be determined from *in-situ* GC-MS results. As shown in Fig. 3-7d, the noise severely affected the detection of CO_2 concentration changes, so that no cyclic trend was observed with charge and discharge processes. In addition, the concentration signal of both CO_2 and H_2 gradually faded with testing time, which is a common problem for GC-MS instrument after working for a long time.

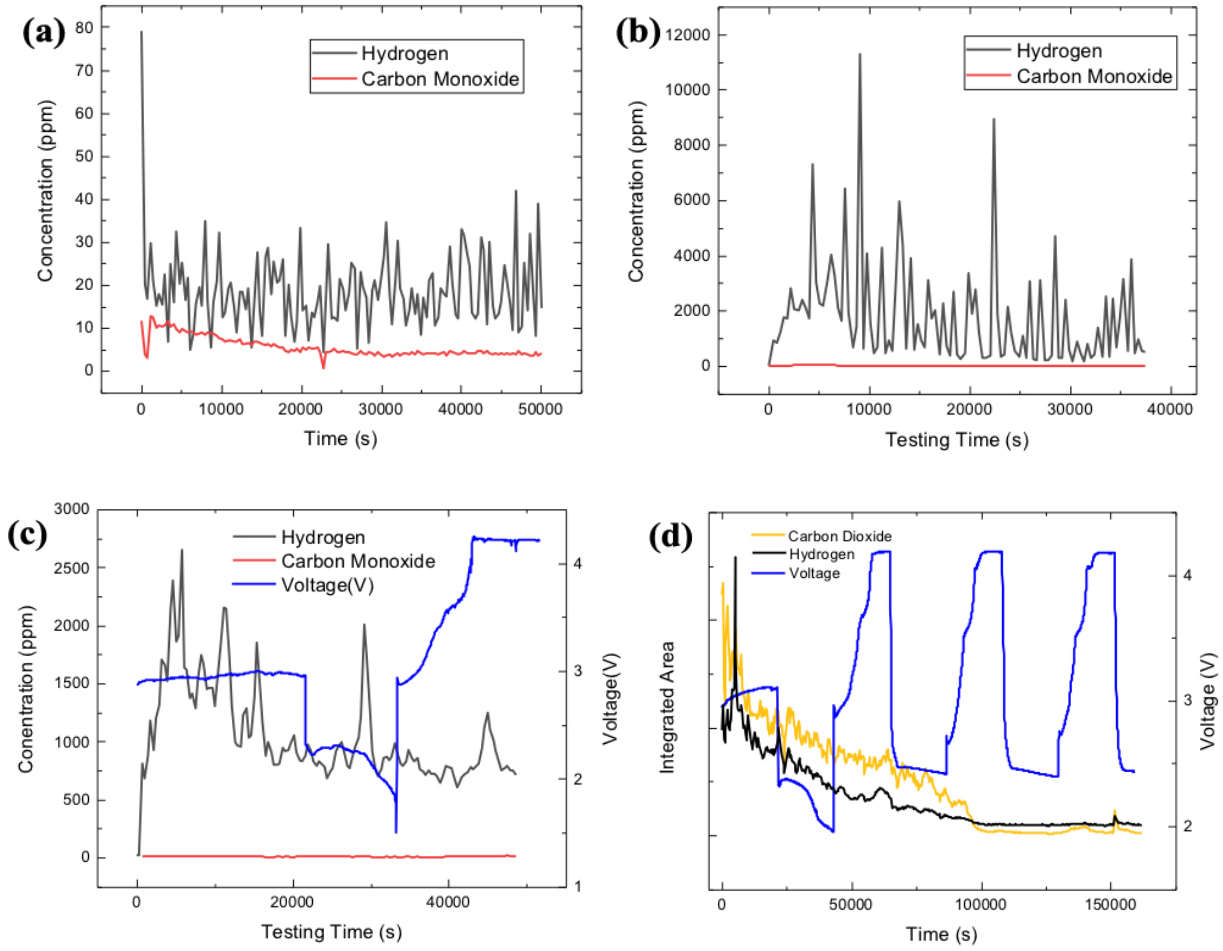

Fig. 3-7. GC-MS results of concentrations of H_2 and CO in (a) the empty battery case, (b) the assembled Li-CO_2 cell without cycling. *In-situ* GC-MS results of concentrations of (c) H_2 and CO, (d) H_2 and CO_2 in the molten salt Li-CO_2 battery during cycling measured and the corresponding voltage. The operation temperature is 150 °C for all the tests.

Considering above factors, we switched to focus only on the charge process instead of both charge and discharge. In this way, if we can "clean up" the battery after discharge, then the generation of CO_2 can be confirmed once CO_2 signal appears during charge. Therefore, we stopped the Li-CO_2 battery after the first discharge and purged Ar gas into the battery to blow

away all the remained gases. After that, we charged back the Li-CO_2 battery with Ar flowing and measured the gas products by *in-situ* GC-MS at the same time. As demonstrated in Fig. 3-8, CO_2 signal was obviously observed, indicating the formation of CO_2 during the charge process.

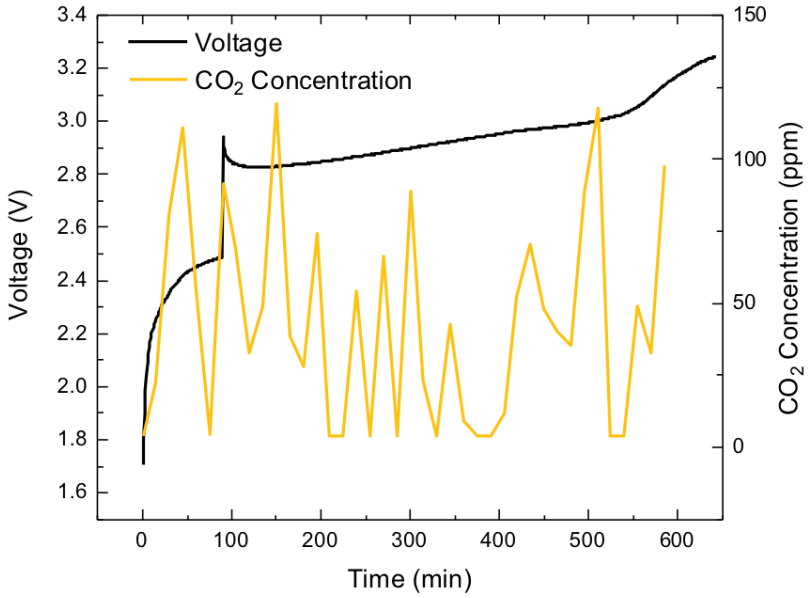

Fig. 3-8. *In-situ* GC-MS results of the concentration of CO_2 in the molten salt Li-CO_2 battery during discharge and the corresponding voltage.

Therefore, the reaction mechanism of molten salt Li-CO_2 batteries can be determined based on both XRD and GC-MS results. The formation of Li_2CO_3 after discharge was confirmed by XRD, while the generation of CO_2 during charge was detected by *in-situ* GC-MS, which should result from the decomposition of Li_2CO_3 and C. The previously purposed reversible discharge/charge reaction[35], which is shown below, can thus be affirmed.

$$4\mathrm{Li} + 3\mathrm{CO_2} \leftrightarrow 2\mathrm{Li_2CO_3} + \mathrm{C}$$

4 Conclusions and Future Work

4.1 Conclusions

As a new type of electrolyte of high thermal and electrochemical stability, nonvolatility, good ionic conductivity, improved working temperature, $LiNO_3$-KNO_3 eutectic molten salt was well applied to Li-O_2 batteries. Together with the noncarbonaceous Ni-nitrate composite cathode, a novel Li-O_2 battery system with stable cycling performance, reasonable capacity and moderate charge/discharge voltage gap was established.

Satisfactory electrochemical performance was also achieved when extending the molten salt Li-O_2 battery system to Li-CO_2 batteries. The Li-CO_2 battery employing identical $LiNO_3$-KNO_3 molten salt electrolyte and Ni-nitrate composite cathode exhibited good cycling performance and specific capacity when operated at 150 °C, which confirms the feasibility of molten salt Li-CO_2 batteries working at improved temperature. More importantly, the solid and gas products generated during charge and discharge processes were tested to verify the purposed reaction mechanism of Li-CO_2 batteries. In such a system without organic electrolytes or carbon cathodes, the existence of Li_2CO_3 on the discharged cathode as well as the formation of CO_2 during charge provide convincing evidences for the purposed reversible reaction mechanism with Li_2CO_3 and C as discharge products. These results can be the foundation for further development of Li-CO_2 batteries and molten salt electrolyte systems.

4.2 Future Work

In-depth investigation and verification are still needed for the new system of molten salt electrolyte Li-gas batteries. The morphology of the electrodes before and after reactions should be characterized by SEM and TEM, as a support for the formation of solid products. Since amorphous carbon cannot be identified by XRD, XPS or Raman analysis can be used to confirm its existence as another discharge product of Li-CO_2 batteries. Some supplementary electrochemical tests can also be conducted, such as cycling at higher current densities, cycling at various rates, impedance measurement.

Furthermore, based on the success of molten salt Li-O_2 and Li-CO_2 batteries, this new system can be applied to more electrochemical redox reactions besides ORR, OER, CO_2 reduction and evolution reactions. For example, we are trying to realize nitrogen reduction reaction (NRR) in the molten salt battery by exploring suitable electrolytes. In this way, the energy storage devices and electrocatalysis systems can be better combined, leading to numerous promising applications.

5 References

1 Goodenough, John B. "Electrochemical energy storage in a sustainable modern society." *Energy & Environmental Science* 7.1 (2014): 14-18.

2 Monconduit, Laure. "Recent advancements in the conversion-type Pnictide-based electrodes for li-ion batteries." *The Journal of Physical Chemistry C* 118.20 (2014): 10531-10544.

3 Sawicki, Monica, and Leon L. Shaw. "Advances and challenges of sodium ion batteries as post lithium ion batteries." *RSC Advances* 5.65 (2015): 53129-53154.

4 Wang, Luyuan Paul, et al. "Recent developments in electrode materials for sodium-ion batteries." *Journal of Materials Chemistry A* 3.18 (2015): 9353-9378.

5 Xie, Zhaojun, et al. "Metal–CO2 batteries on the road: CO2 from contamination gas to energy source." *Advanced Materials* 29.15 (2017): 1605891.

6 Xie, Jiafang, and Yaobing Wang. "Recent Development of CO2 Electrochemistry from Li–CO2 Batteries to Zn–CO2 Batteries." *Accounts of chemical research* 52.6 (2019): 1721-1729.

7 Giordani, Vincent, et al. "A molten salt lithium–oxygen battery." *Journal of the American Chemical Society* 138.8 (2016): 2656-2663.

8 Cai, Kedi, et al. "Investigation of technology for lithium-oxygen battery." *Progress in Chemistry* 27.12 (2015): 1722-1731.

9 Lu, Yi-Chun, et al. "Lithium–oxygen batteries: bridging mechanistic understanding and battery performance." *Energy & Environmental Science* 6.3 (2013): 750-768.

10 Abraham, K. M., and Z. Jiang. "A polymer electrolyte-based rechargeable lithium/oxygen

battery." *Journal of The Electrochemical Society* 143.1 (1996): 1-5.

11 Zhang, Sheng S., Donald Foster, and Jeffrey Read. "Discharge characteristic of a non-aqueous electrolyte Li/O2 battery." *Journal of Power Sources* 195.4 (2010): 1235-1240.

12 McCloskey, Bryan D., et al. "Solvents' critical role in nonaqueous lithium–oxygen battery electrochemistry." *The Journal of Physical Chemistry Letters* 2.10 (2011): 1161-1166.

13 Laoire, Cormac O., et al. "Influence of nonaqueous solvents on the electrochemistry of oxygen in the rechargeable lithium− air battery." *The Journal of Physical Chemistry C* 114.19 (2010): 9178-9186.

14 Allen, Chris J., et al. "Oxygen reduction reactions in ionic liquids and the formulation of a general ORR mechanism for Li–air batteries." *The Journal of Physical Chemistry C* 116.39 (2012): 20755-20764.

15 Miles, M. H., and A. N. Fletcher. "Cation effects on the electrode reduction of molten nitrates." *Journal of The Electrochemical Society* 127.8 (1980): 1761.

16 Zambonin, Pier Giorgio. "Reversible oxygen electrode systems in molten salts." *Journal of Electroanalytical Chemistry and Interfacial Electrochemistry* 33.2 (1971): 243-251.

17 Zambonin, Pier G., and Joseph Jordan. "Redox chemistry of the system O2-O2--O22--O2-in fused salts." *Journal of the American Chemical Society* 91.9 (1969): 2225-2228.

18 Karkera, Guruprakash, and A. S. Prakash. "An Inorganic Electrolyte Li–O2 Battery with High Rate and Improved Performance." *ACS Applied Energy Materials* 1.3 (2018): 1381-1388.

19 Mo, Yifei, Shyue Ping Ong, and Gerbrand Ceder. "First-principles study of the oxygen evolution reaction of lithium peroxide in the lithium-air battery." *Physical Review B* 84.20

(2011): 205446.

20 Radin, Maxwell D., et al. "Lithium peroxide surfaces are metallic, while lithium oxide surfaces are not." *Journal of the American Chemical Society* 134.2 (2012): 1093-1103.

21 Giordani, Vincent, et al. "High concentration lithium nitrate/dimethylacetamide electrolytes for lithium/oxygen cells." *Journal of The Electrochemical Society* 163.13 (2016): A2673.

22 Yao, Xiahui, et al. "Why do lithium–oxygen batteries fail: parasitic chemical reactions and their synergistic effect." *Angewandte Chemie International Edition* 55.38 (2016): 11344-11353.

23 Xia, C. Y. K. C., C. Y. Kwok, and L. F. Nazar. "A high-energy-density lithium-oxygen battery based on a reversible four-electron conversion to lithium oxide." *Science* 361.6404 (2018): 777-781.

24 Adams, Brian D., et al. "Current density dependence of peroxide formation in the Li–O 2 battery and its effect on charge." *Energy & Environmental Science* 6.6 (2013): 1772-1778.

25 Feng, Shuting, et al. "Hot lithium-oxygen batteries charge ahead." *Science* 361.6404 (2018): 758-758.

26 Li, Xiang, et al. "Progress in research on Li–CO2 batteries: Mechanism, catalyst and performance." *Chinese Journal of Catalysis* 37.7 (2016): 1016-1024.

27 Qiao, Yu, et al. "Li-CO2 electrochemistry: a new strategy for CO2 fixation and energy storage." *Joule* 1.2 (2017): 359-370.

28 Takechi, Kensuke, Tohru Shiga, and Takahiko Asaoka. "A li–o 2/co 2 battery." *Chemical Communications* 47.12 (2011): 3463-3465.

29 Gowda, Sanketh R., et al. "Implications of CO2 contamination in rechargeable nonaqueous Li–O2 batteries." *The journal of physical chemistry letters* 4.2 (2013): 276-279.

30 Mekonnen, Yedilfana S., et al. "Communication: The influence of CO2 poisoning on overvoltages and discharge capacity in non-aqueous Li-Air batteries." *The Journal of Chemical Physics* 140 (2014): 121101.

31 McCloskey, Bryan D., et al. "Solvents' critical role in nonaqueous lithium–oxygen battery electrochemistry." *The Journal of Physical Chemistry Letters* 2.10 (2011): 1161-1166.

32 Lim, Hyung-Kyu, et al. "Toward a lithium–"air" battery: the effect of CO2 on the chemistry of a lithium–oxygen cell." *Journal of the American Chemical Society* 135.26 (2013): 9733-9742.

33 Sharon, Daniel, et al. "Oxidation of dimethyl sulfoxide solutions by electrochemical reduction of oxygen." *The Journal of Physical Chemistry Letters* 4.18 (2013): 3115-3119.

34 Kwabi, David G., et al. "Chemical instability of dimethyl sulfoxide in lithium–air batteries." *The journal of physical chemistry letters* 5.16 (2014): 2850-2856.

35 Liu, Yali, et al. "Rechargeable Li/CO 2–O 2 (2: 1) battery and Li/CO 2 battery." *Energy & Environmental Science* 7.2 (2014): 677-681.

36 Xu, Shaomao, Shyamal K. Das, and Lynden A. Archer. "The Li–CO 2 battery: A novel method for CO 2 capture and utilization." *RSC Advances* 3.18 (2013): 6656-6660.

37 Das, Shyamal K., et al. "High energy lithium–oxygen batteries–transport barriers and thermodynamics." *Energy & Environmental Science* 5.10 (2012): 8927-8931.

38 Su, Liwei, et al. "CoCO3 submicrocube/graphene composites with high lithium storage capability." *Nano Energy* 2.2 (2013): 276-282.

39 Zhang, Zhang, et al. "The first introduction of graphene to rechargeable Li–CO2 batteries." *Angewandte Chemie International Edition* 54.22 (2015): 6550-6553.

40 Zhang, Zhang, et al. "Identification of cathode stability in Li–CO 2 batteries with Cu nanoparticles highly dispersed on N-doped graphene." *Journal of Materials Chemistry A* 6.7 (2018): 3218-3223.

41 Zhang, Xin, et al. "Rechargeable Li–CO2 batteries with carbon nanotubes as air cathodes." *Chemical Communications* 51.78 (2015): 14636-14639.

42 Zhao, Huimin, et al. "Ru nanosheet catalyst supported by three-dimensional nickel foam as a binder-free cathode for Li–CO2 batteries." *Electrochimica Acta* 299 (2019): 592-599.

43 Hou, Yuyang, et al. "Mo2C/CNT: an efficient catalyst for rechargeable Li–CO2 batteries." *Advanced Functional Materials* 27.27 (2017): 1700564.

44 Zhou, Jingwen, et al. "A quasi-solid-state flexible fiber-shaped Li–CO2 battery with low overpotential and high energy efficiency." *Advanced Materials* 31.3 (2019): 1804439.

45 Németh, Károly, and George Srajer. "CO 2/oxalate cathodes as safe and efficient alternatives in high energy density metal–air type rechargeable batteries." *RSC Advances* 4.4 (2014): 1879-1885.

46 Royal Society of Chemistry, *Periodic Table* <https://www.rsc.org/periodic-table/element/3/lithium>.

47 Zhang, Xuejun, Kangcheng Xu, and Yici Gao. "The phase diagram of LiNO3–KNO3." *Thermochimica acta* 385.1-2 (2002): 81-84.

48 Yang, Sixie, et al. "A reversible lithium–CO 2 battery with Ru nanoparticles as a cathode

catalyst." *Energy & Environmental Science* 10.4 (2017): 972-978.

Hanqian Zhi

Tel: +1 4435007260; **Email**: hzhi2@jhu.edu
500 W. University Pkwy, Apt. 12C, Baltimore, MD, 21210

EDUCATION

08/2018 – 05/2020 **Johns Hopkins University (JHU)**, Baltimore, MD, USA
Major: Materials Science and Engineering (M.S.E.)

09/2014 – 06/2018 **Fudan University (FDU)**, Shanghai, China
Major: Materials Chemistry (B.S.)

RESEARCH EXPERIENCE

01/2019 – 05/2020 **Tuning Lithium Insertion Sn Alloy for CO_2 Reduction Reaction**

- Established a novel system preparing electrocatalyst through batteries.
- Discharged SnO_2 lithium ion batteries to different cutoff voltages; analyzed the CO_2 reduction reaction performance of formed Li-Sn alloys with various crystal structures by GDE cells; determined the alloy with best performance; confirmed the surface reaction mechanism.
- Proved Li-Sn alloys formation by ICP analysis; acquired product distributions by GC-MS and NMR.
- Extended the system to other transition metals and oxides.

09/2018 – 05/2020 **Molten Salt Electrolyte Lithium-Gas Batteries**

- Conducted a high-temperature Li-O_2 battery system by replacing traditional organic electrolyte with molten salt mixture; prepared battery components including Ni-nitrate cathodes, nitrites soaked glass fibers, LAGP solid electrolyte membranes; assembled batteries in the glovebox.
- Carried out electrochemical tests of charge-discharge cycling and CV; measured products by *in situ* GC-MS; identified solid products by XRD; analyzed ORR and OER in such system.
- Realized Li-CO_2 batteries based on molten salt Li-O_2 batteries; studied their reaction mechanism.

12/2016 – 06/2018 **Nanostructured Ni_2P/C Composites as Anode Materials for Sodium Ion Batteries**

- Prepared 40-60 nm Ni_2P nanoparticles and nanofibers by solvothermal reaction and electrospinning; improved the capacity by 70% through carbon modification, 35% higher than the literature value.
- Received ¥10,000 financial support from FDUROP Wangdao Project; honored as "Wangdao Scholar".
- Took charge of materials synthesis, electrochemical tests and materials characterization such as SEM, TEM, XRD, cycling, rate and impedance tests, CV.

PUBLICATION

- Liu W, **Zhi H**, Yu X (2019). Recent progress in phosphorus based anode materials for lithium/sodium ion batteries. *Energy Storage Materials*. 290(16).

INTERNSHIP EXPERIENCE

12/2019 – 03/2020 **The Lubrizol Corporation**, *Product Compliance Intern*

- Completed relevant documents for product declaration in Korea, Thailand, Japan, Europe and other regions using SAP, SDS and internal records; updated and organized new records.
- Issued more than 400 Letters of Confirmation (LoCs); submitted over 200 100% composition forms;

checked First Time Shipment Report (FTSR) daily; coordinated with Korea colleagues.

- Disclosed monomer information of imported polymer products to customs through data mining; shortened the declaration time up to 7 days.

10/2019 – 04/2020 **iWeekly Magazine**, *Overseas Part-time Author*

- Wrote articles related to international news during 11 p.m. to 8 a.m.; selected 3 topics each time; read an average of 10 news and 5 materials for each article.
- Published more than 60 articles on WeChat official account and app with highest 10,000+ readings.

07/2017 – 08/2017 **Shanghai Baosteel Chemical Co., Ltd.**, Planning and Investment Department, *Intern*

- Based on the feasibility study report of "Tar DeepProcessing 100,000 tons/year Modified Asphalt Project", did literature review with more than 80 articles and analyzed the development status of biodiesel in different regions from ingredients, processes, equipment, policies, etc.
- Converted obtained results into a report; got it used as the introduction part of new project.

EXTRACURRICULAR ACTIVITIES

03/2015 – 06/2015 **FDU Interest-Sharing Groups**, *Founder*

- Aimed at sharing of interest and skills through online videos, amateur coaches, experience sharing, etc.; provided online and offline teaching resources and communication platform for participants.
- Organized respondents' needs through over 200 effective questionnaires; established 5 groups of football, baking, guitar, makeup, and aerobics; attracted 60+ participants and 130+ Wechat followers.
- Wrote WeChat articles for activities promotion; planned the project schedule by Gantt chart; summarized achievements and limitations during activities; collected feedback from participants.

09/2014 – 06/2018 **FDU Unilever Club**, *HR Member*

- Undertook activities supervision and personnel evaluation; assisted in annual Unilever campus talk.

09/2014 – 06/2016 **FDU Self-Discipline Association (SDA) of Xide College**, *Deputy Minister*

- Led the team in planning and supervising activities within SDA including ice breaking, built-in, year-end summary conference; developed the personnel evaluation to an interesting quiz.
- Held college-level activities including Carnival (more than 400 participants), chamber escape, time capsule, handmade DIY etc.; designed the process of activities; prepared promotional products, such as posters, roll-ups, flyers, H5 pages; wrote articles for the WeChat official account.

09/2014 – 06/2015 **FDU Student Union, Outreach Department**, Inter-school Exchange Section, *Member*

- Negotiated with the outreach department of other universities to co-organize inter-school activities.
- Coordinated in the first Shanghai University Public Relations and Outreach Development Summit.

SKILLS & SPECIALTY

- **Languages**: Native speaker of Mandarin Chinese; Fluent in English
- **Software**: Frequent user of Microsoft Office, Origin; Familiar with Photoshop, SAP database
- **Computer Skills**: Basic C Language Programming, MATLAB
- **Hobbies**: Writing; watercolor painting; Zheng (Chinese zither) (Amateur Grade 4)